

# Connected macroalgal-sediment systems: blue carbon and food webs in the deep coastal ocean

ANA MOURA QUEIRÓS <sup>1,7</sup>, NICHOLAS STEPHENS <sup>1,2</sup>, STEPHEN WIDDICOMBE <sup>1</sup>, KAREN TAIT <sup>1</sup>,  
SOPHIE J. MCCOY <sup>1,3</sup>, JEROEN INGELS <sup>1,4</sup>, SASKIA RÜHL,<sup>1</sup> RUTH AIRS <sup>1</sup>, AMANDA BEESLEY,<sup>1</sup> GIORGIA  
CARNOVALE,<sup>1</sup> PIERRE CAZENAVE <sup>1</sup>, SARAH DASHFIELD,<sup>1</sup> ER HUA <sup>1,5</sup>, MARK JONES,<sup>1</sup> PENELOPE LINDEQUE <sup>1</sup>,  
CAROLINE L. MCNEILL,<sup>1</sup> JOANA NUNES,<sup>1</sup> HELEN PARRY,<sup>1</sup> CHRISTINE PASCOE,<sup>1</sup> CLAIRE WIDDICOMBE <sup>1</sup>,  
TIM SMYTH <sup>1</sup>, ANGUS ATKINSON <sup>1</sup>, DORTE KRAUSE-JENSEN <sup>1,6</sup> AND PAUL J. SOMERFIELD <sup>1</sup>

<sup>1</sup>Plymouth Marine Laboratory, Plymouth PL1 3DH United Kingdom

<sup>2</sup>Nereis Bioengineering, Llansadwrn SA19 8NA United Kingdom

<sup>3</sup>Department of Biological Science, Florida State University, Tallahassee, Florida 32306 USA

<sup>4</sup>Coastal and Marine Laboratory, Florida State University, St Teresa, Florida 32358 USA

<sup>5</sup>Ocean University of China, Qingdao 266003 China

<sup>6</sup>Aarhus University, Silkeborg 8600 Denmark

*Citation:* Moura Queirós, A., N. Stephens, S. Widdicombe, K. Tait, S. J. McCoy, J. Ingels, S. Rühl, R. Airs, A. Beesley, G. Carnovale, P. Cazenave, S. Dashfield, E. Hua, M. Jones, P. Lindeque, C. L. McNeill, J. Nunes, H. Parry, C. Pascoe, C. Widdicombe, T. Smyth, A. Atkinson, D. Krause-Jensen, and P. J. Somerfield. 2019. Connected macroalgal-sediment systems: blue carbon and food webs in the deep coastal ocean. *Ecological Monographs* 00(00):e01366. 10.1002/ecm.1366

*Abstract.* Macroalgae drive the largest CO<sub>2</sub> flux fixed globally by marine macrophytes. Most of the resulting biomass is exported through the coastal ocean as detritus and yet almost no field measurements have verified its potential net sequestration in marine sediments. This gap limits the scope for the inclusion of macroalgae within blue carbon schemes that support ocean carbon sequestration globally, and the understanding of the role their carbon plays within distal food webs. Here, we pursued three lines of evidence (eDNA sequencing, Bayesian Stable Isotope Mixing Modeling, and benthic-pelagic process measurements) to generate needed, novel data addressing this gap. To this end, a 13-month study was undertaken at a deep coastal sedimentary site in the English Channel, and the surrounding shoreline of Plymouth, UK. The eDNA sequencing indicated that detritus from most macroalgae in surrounding shores occurs within deep, coastal sediments, with detritus supply reflecting the seasonal ecology of individual species. Bayesian stable isotope mixing modeling [C and N] highlighted its vital role in supporting the deep coastal benthic food web (22–36% of diets), especially when other resources are seasonally low. The magnitude of detritus uptake within the food web and sediments varies seasonally, with an average net sedimentary organic macroalgal carbon sequestration of 8.75 g C·m<sup>-2</sup>·yr<sup>-1</sup>. The average net sequestration of particulate organic carbon in sediments is 58.74 g C·m<sup>-2</sup>·yr<sup>-1</sup>, the two rates corresponding to 4–5% and 26–37% of those associated with mangroves, salt marshes, and seagrass beds, systems more readily identified as blue carbon habitats. These novel data provide important first estimates that help to contextualize the importance of macroalgal-sedimentary connectivity for deep coastal food webs, and measured fluxes help constrain its role within global blue carbon that can support policy development. At a time when climate change mitigation is at the foreground of environmental policy development, embracing the full potential of the ocean in supporting climate regulation *via* CO<sub>2</sub> sequestration is a necessity.

*Key words:* benthos; blue carbon; carbon cycling; climate change; ecosystem connectivity; food web; macrophyte; mitigation; Paris Agreement; trophic subsidy.

## INTRODUCTION

The 2015 Paris Agreement has been ratified by 195 parties. If successfully implemented, it sets the world on

Manuscript received 9 June 2018; revised 19 November 2018; accepted 7 January 2019. Corresponding Editor: Michael H. Graham.

<sup>7</sup>E-mail: anqu@pml.ac.uk

a course to avoid average global warming above 2°C, through a reduction of carbon dioxide and other greenhouse gas emissions. We understand that the ocean should be part of this process, as a vital regulator of the global carbon cycle and housing major stores of carbon (Le Quéré et al. 2016). Indeed, the potential for improved management of these “blue carbon” stores and habitats to reduce CO<sub>2</sub> emissions has been recognized

within National Determined Contributions; that is, national commitments made within the agreement, and there is potential to expand these actions (Gallo et al. 2017, Macreadie et al. 2017). The term “blue carbon” refers to carbon sequestration in the ocean, primarily by vegetated coastal habitats including mangroves, seagrass beds, and salt marshes, where atmospheric CO<sub>2</sub> is fixed as part of a stable living biomass store, and organic matter trapped within sediments provides long-term storage (McLeod et al. 2011). Nowhere else in the coastal and open ocean is the full blue carbon cycle (from fixing of CO<sub>2</sub> to permanent sequestration) known to occur within single habitats (Nellemann et al. 2009, Duarte et al. 2013, Howard et al. 2017). Therefore, initiatives that strive for the conservation of blue carbon have not often considered other ocean or coastal habitats (Howard et al. 2017, Krause-Jensen et al. 2018). In the Dominican Republic, Vanuatu, and elsewhere, Nationally Appropriate Mitigation Actions and other policy frameworks seeking to limit greenhouse gas emissions and global climate change through ocean conservation have thus primarily focused on protecting these three habitats (Laffoley 2013, Hejnowicz et al. 2015).

However, in the context of the global carbon cycle, other habitats and ecosystem components exist that represent important steps of the blue carbon delivered by the global ocean. For instance, macroalgae have large standing biomass and production rates. With a much wider global distribution than mangroves, seagrass beds, and salt marshes, macroalgae are thus the most productive marine macrophytes at the global scale, and it has long been suggested that they make a large contribution to the global C sink (Smith 1981, Duarte and Cebrián 1996, Gattuso et al. 2006). Because macroalgae occur predominantly on rocky shorelines and shallow reefs, where there is limited potential for storage of organic carbon, up to 80% of the organic carbon they fix can be seasonally exported (Krumhansl and Scheibling 2012). Indeed, of the estimated 1,521 Tg C/yr global net primary production of macroalgae, it is estimated that 323 Tg C/yr are exported from shorelines as particulate organic carbon, with 89% of this material assumed to stay in the coastal ocean (reviewed by Krause-Jensen and Duarte 2016). Further estimates of what fractions of this carbon are sequestered or re-mineralized coastally are largely missing, with existing data derived from laboratorial studies; in situ measurements are virtually absent. The fate of this carbon is therefore largely unknown, raising important questions concerning transport mechanisms, whether and where it becomes sequestered, and if so, at what rate (Krause-Jensen and Duarte 2016). We know that through this and similar processes, the land–ocean continuum contributes to the net annual growth of long-term open ocean carbon storage in marine sediments (Regnier et al. 2013). But large uncertainty remains around the actual size of these fluxes, as well as the identity and magnitude of all the processes contributing to them (Le Quéré et al. 2016). Measuring

and managing the whole blue carbon capacity of the global ocean, to maximize the use of this natural storage toward reduced CO<sub>2</sub> emissions, therefore requires a stepped improvement in our understanding of the connectivity between the individual ocean components that deliver the various parts of global blue carbon, in addition to that delivered by coastal vegetated habitats (Polis et al. 1997, Smale et al. 2018).

Meeting these objectives requires a wider scope than simply estimating the accumulation of macroalgal and other organic carbon on the seabed (i.e., sedimentation). Specifically, a more comprehensive quantification of the fraction of that carbon that is retained by the benthic compartment, over the seasonal cycle, requires the consideration of processes mediated by benthic faunal communities (Snelgrove et al. 2018, Lessin et al. 2018). Carbon sequestration on the seafloor is usually inferred from field measurements and modeling that consider sedimentation rates and other physical processes. Most often, these approaches neglect the vital role that seabed organisms play in determining influx and efflux of carbon at the sediment–water interface, and their contributions toward net carbon sequestration (Middelburg 2018, Snelgrove et al. 2018). These processes include: active flushing of the seabed via bioirrigation (which promotes the uptake of solutes and suspended particles; Kristensen et al. 2012); active transport of particulates *via* bioturbation (Kristensen et al. 2012), which will promote the uptake of organic matter deposited at the surface of sediments at depth; and the large effect on carbon mineralization rates driven by sedimentary community respiration (Glud 2008). The importance of these globally relevant processes (Snelgrove et al. 2018), which occur throughout 80% of the ocean seafloor (Byers and Grabowski 2014) and largely outside of fringe habitats such as wetlands, has not been recognized in the context of blue carbon, and especially not in the context of blue carbon in an organic carbon donor and sink framework (Polis et al. 1997, Hill et al. 2015, Smale et al. 2018). It is therefore likely that blue carbon estimates that have neglected these processes may underestimate globally relevant carbon exchanges at the seabed surface (Burrows et al. 2014) and ignore ecosystem components involved in this exchange. The role of macroalgal beds in supporting proximal food webs is well documented (Graham 2004); understanding their wider connectivity to distal food webs, and benthic processes within these, is now needed to unravel connectivity processes underpinning global blue carbon (Hill et al. 2015, Smale et al. 2018).

Here, we address these questions focusing on one of the most comprehensively studied coastal benthic-pelagic systems in the world: Station L4, off of Plymouth in the Western English Channel (Smyth et al. 2015). During a 13-month research program, we combined environmental DNA (eDNA) sequencing (Bohmann et al. 2014) and Bayesian Mixing Modeling of bulk stable isotope data (Phillips et al. 2014) as complementary bio-tracing techniques (Nielsen et al. 2018) with direct

benthic-pelagic process measurements, to investigate three questions: (1) Can macroalgal detritus be found on the seafloor of the deep coastal ocean? (2) If so, how important is macroalgal detritus to the coastal benthic marine food web, relative to other carbon sources? (3) What is the net sequestration of organic macroalgal carbon in these coastal, deep sediments? We employ the term “deep” throughout referring to coastal sediments that occur in the deeper, subtidal regions of the coastal ocean, outside of coastal vegetated habitats.

The linkage of the benthic community at the Station L4 to phytoplankton phenology has been previously documented, and the basic phenology of coastal macroalgal detritus export has been investigated (Queirós et al. 2015b, Smale and Vance 2015, Zhang et al. 2015). Furthermore, that this macroalgal detritus may make a potentially important contribution to organic detritus reaching the seabed at L4 was suggested almost a century ago (Hunt 1925). However, at Station L4 as in the majority of the world’s ocean, we had no understanding of whether it did, or what role this organic carbon may play in supporting the coastal benthic food web and blue carbon. For instance, rafts of reproductive fronds of macroalgae such as *Himantalia elongata* (Linnaeus) are routinely observed on the water surface near and beyond Station L4 (Queirós, personal observation), but the exact location of their shore of origin, or the potential fate of their organic carbon is unknown. We hypothesized that the large export of detritus from local macroalgal beds (Smale and Vance 2015) may represent an important source of organic detritus to the L4 sedimentary system, especially during winter months, when plankton biomass is low (Smyth et al. 2015) and storm-driven macroalgal biomass loss from the shore may be most significant. This study aimed to provide a first basis quantification of the connectivity between macroalgal beds and sedimentary systems in the deep coastal ocean.

## MATERIALS AND METHODS

### *A seasonal program*

The sampling program took place over seven time points (May, July, September, and November 2015, and January, March, and May 2016); it is summarized as a schematic diagram in Appendix S1: Fig. S1. At each time point, shore surveys of macroalgal beds around Plymouth Sound were complemented by sampling at Station L4 (Fig. 1) on board Plymouth Marine Laboratory’s RV Plymouth Quest and associated, lab-based benthic-pelagic process measurements. Stable isotope tracing studies are influenced by spatial and temporal variations in the isotopic values of both sources and consumers (Miller and Page 2012, Dethier et al. 2013, Kopp et al. 2015) and this has been identified as a challenge in studies tracing macroalgal carbon (Hill et al. 2015). We avoided this challenge by fixing our sampling locations

to limit spatial confounding and undertaking a finely resolved seasonal sampling program to characterize temporal variability in the processes and variables assessed in this study. This variability was taken into account throughout our analyses.

### *Shore surveys*

As in the rest of the global ocean, we did not initially know the precise hydrodynamic path of macroalgal detritus transport between the shores bordering Plymouth Sound and the sampled sediments at Station L4. We therefore selected two macroalgal shore communities that were potentially suitably placed geographically to generate detritus that could reach Station L4 through surface and water column transport (Fig. 1; Krause-Jensen and Duarte 2016). Sampling more than one macroalgal community was important because location can affect the elemental and isotopic characterization of individuals, which affects Bayesian Stable Isotope Mixing Modeling (Phillips et al. 2014). The two sites sampled were Rame Head (50°18′41.9″ N 4°13′15.9″ W) and Plymouth Hoe (50°21′49.3″ N 4°08′28.9″ W; Fig. 1).



FIG. 1. The Western Channel Observatory, UK, showing the main sampling sites in this study (Station L4 and its associated benthic monitoring site), as well as the coastal macroalgae sampling sites (Plymouth Hoe and Rame Head). The bathymetry shown was interpolated to 10-m resolution from the United Kingdom Hydrographic Office’s sounding, single-beam, and multi-beam data.

Based on records held for the region by the UK Archive for Marine Species and Habitats Data at the start of the study (September 2014) we sampled the dominant coastal macroalgal species in the intertidal and fringe subtidal (*Laminaria hyperborea* (Gunnerus), *Saccharina latissima* (Linnaeus), *Fucus serratus* (Linnaeus) and *Himantalia elongata* (Linnaeus)). On each sampling occasion, tissue samples were collected by hand at low water, from three distinct individuals per species. These samples we used in subsequent elemental and stable isotope analyses. The technique used for sample collection is described in Appendix S2. This sampling was combined with literature searches on each species life-history to define a preliminary seasonality for detritus export.

### Seabed sampling

Coastal soft sediments were sampled from Station L4's benthic monitoring site (50°13'22.7" N 4°11'23.0" W, Fig. 1, also known as Hilmar's Box). This site is located 13 km south-southwest of Plymouth, off Plymouth Sound, and is approximately 48 m deep (Smyth et al. 2015). The seabed is characterized as sandy mud (Queirós et al. 2015b). The sediment surface is covered by a bottom water layer of varying thickness comprised of detritus, fine sediment, and living organisms, that is flushed and resettled within the tidal cycle (the "fluff layer"). General hydrological conditions of the site are characterized by a combination of the coastal influence of the Tamar estuary, and water column thermal stratification typically observed in the UK continental shelf during summer months (Smyth et al. 2015). On each date, sampling was undertaken as close as possible to slack water after high tide, to maximize the ability to capture the fluff layer. On each occasion, four cores (10.5 cm inner diameter) were collected from four separate deployments of a multi-corer to support the stable isotope and eDNA work. Although the multi-corer collects four cores simultaneously, we used only one core from each deployment to reduce the risk of changes to measured pools and processes during waiting time on deck reflecting core processing, and to improve the spatial coverage of the samples collected at each time point. This gear retrieves a sediment core (~15 cm deep) and seals the bottom water above it (~70 cm column) preserving the structural integrity of the core and sediment water interface during retrieval to the deck. Additionally, eight squared sediment cores (12 × 12 cm inner diameter) were collected during each sampling trip, using four separate deployments of a US-NL box corer (Plymouth Marine Laboratory, Plymouth, UK) (two paired squared cores per deployment, 0.1 m<sup>2</sup>), taking care to preserve the water layer above the sediment. These squared cores had the bottoms immediately sealed on deck, and were individually aerated and kept cool and shaded during transport to Plymouth Marine Laboratory for benthic-pelagic process measurements. A CTD was deployed midway through each sampling day

(Rosette mounted SeaBird sensors SBE 19 plus and ancillary dissolved oxygen sensor SBE 43, Plymouth Marine Laboratory, Plymouth, UK) to acquire temperature, salinity, and dissolved oxygen depth profiles.

*Deck processing of multi-cores: water samples.*—Once on deck, the temperature of the water in each corer tube was immediately recorded with a digital thermometer. The water at the top of each corer tube (70 cm above the sediment water interface, hereafter, top water) was sampled to determine the  $\delta^{13}\text{C}$  of dissolved inorganic carbon (DIC), and  $\delta^{13}\text{C}$ ,  $\delta^{15}\text{N}$ , total particulate carbon (TPC), particulate organic carbon (POC), and total particulate nitrogen (TPN) content of suspended particulate organic matter (SPOM). These measurements were repeated in the fluff layer, as both layers were considered to contain material immediately available to the benthos at the sediment–water interface. The water within the fluff layer was visibly distinct from the remaining bottom water column due to the high concentration of suspended material (organic and inorganic, data not shown).

Within both water layers in each multi-core, the  $\delta^{13}\text{C}$  of DIC was determined from  $\Sigma\text{CO}_2$  evolved by acidification in a Helium gas headspace. Details of this technique are provided in Appendix S2. Exetainers (Labco, Lampeter, UK) treated in the same way but onto which no sample was injected (hereafter, control) were exposed to the same transport and preservation conditions as the samples and were used to assess sample contamination with atmospheric  $\text{CO}_2$  during storage (6 months maximum). DIC water samples and controls were kept at 4°C in a dark fridge until processing, with Exetainers positioned cap side down to reduce the potential for sample contamination through diffusion of atmospheric  $\text{CO}_2$  via the newly perforated cap septum (Waldron et al. 2014).

Suspended particulate organic matter samples from both water layers in each multi-corer tube were acquired through on-deck filtering of tube water onto GF/F grade filters that had been prepared by combustion (425°C, Fisher). Each of the two water samples was gently flushed through the filter using a vacuum pump and pre-acid-washed glass filter holders, until no more water could be filtered (i.e., the filter became clogged). The remaining water in the vacuum funnel was then gently syphoned off and the water volume filtered was recorded. These values were used to help determine the concentration of POC in suspension near the seabed, within each of the two water layers. These, in turn, were used in subsequent net organic carbon sequestration and blue carbon sequestration calculations. Each filter was immediately removed into a new, sterile Petri dish, which was closed and covered in foil to avoid photo-degradation, and preserved upright at –20°C until processing. SPOM collected at 70 cm above the sediment was included in the Bayesian stable isotope mixing model analyses as a potential organic matter source, to capture any potential organic material of diffuse origin that may have been available to the seabed (e.g., derived from the Tamar estuary) in addition to the

pure sources we targeted explicitly (macroalgae, and phyto- and zooplankton).

*Processing of multi-cores: sediment and fauna samples.*—After water sampling, the remaining water in each corer tube was gently syphoned off and discarded, avoiding disturbance to the sediment–water interface. Each multicorer tube was then mounted onto a custom-built core slicer for processing. A 2.5-mL sterile syringe (0.5 cm inner diameter, 0.6 mL), which had the bottom cut off, was used to collect the top 1 cm of sediment. This section would then be used to assess the presence of macroalgae using eDNA sequencing. The sampled sediment was immediately transferred into a sterile Eppendorf tip and frozen in liquid nitrogen until retrieval to the laboratory, where it was stored at  $-80^{\circ}\text{C}$  until processing.

The remaining material in the top 2-cm layer of each core was then sliced and sampled for meiofauna, macrofauna, and bulk sediment (BSed). A 50-mL pre-acid-washed and autoclaved syringe, which had the bottom cut off, was used to sample meiofauna (13 mL) and the sediment transferred into a pre-acid-washed and autoclaved 50-mL falcon tube. The same syringe was used to collect BSed, using the same type of falcon tube. The remaining surficial sediment slice (150 mL) was transferred to a pre-acid-washed and autoclaved sealable glass jar, which was kept cool using a cooling box and ice packs during transport to the laboratory. This sediment sample would be used for macrofauna assessments. This sampling procedure was repeated in deeper sediment layers, 2–6 cm depth and 6–10 cm depth, from which BSed (26 mL) and macrofaunal samples (354 mL) were also collected.

Samples were returned to Plymouth Marine Laboratory (typically, four to six hours later) where all meiofauna and BSed samples were frozen at  $-20^{\circ}\text{C}$  until processing. Conversely, each macrofaunal sample was kept at  $4^{\circ}\text{C}$ , and manually sorted under a dissection microscope within the following 24 h. This procedure avoided isotopic degradation that results from bulk preservation of macrofauna within sediments (Dannheim et al. 2007). All individuals were picked, taxonomically identified, fresh weighed, and frozen in MilliQ water at  $-80^{\circ}\text{C}$  until further processing, using glassware and tools that had been prepared through acid wash and autoclaving. Resulting taxonomic lists per sample were cross-referenced with the World Register of Marine Species and additional literature searches to establish feeding modes, and thus functional changes in the community over the year that could explain changes in resource use (data available online).<sup>8</sup>

*Sampling of plankton communities as organic carbon resources.*—In addition to onshore macroalgae and offshore SPOM, we also collected samples to isotopically

characterize plankton at Station L4 (main site,  $50^{\circ}15'0.0''$  N  $4^{\circ}13'12.0''$  W, Fig. 1), which is a known food source to the studied coastal sediments. Phyto- and zooplankton communities in the water column at Station L4 were therefore sampled within two weeks of each of the Station L4 sediment sampling occasions. Samples were collected on board the RV Plymouth Quest using Apstein (20  $\mu\text{m}$ ) and WP2 (200  $\mu\text{m}$ ) nets, respectively. Nets were cast to 20 m and 48 m depth, respectively, and hauled vertically at  $\sim 20$  cm/s to the surface, from a stationary ship. This ensured that we sampled the isotopic signal from actively growing phytoplankton in the upper mixed layer (Apstein net) as well as that from mesozooplankton, which can actively transit the whole water column (WP2 net). The cod end contents were concentrated on deck using clean, plexiglas, mesh-bottomed sieves of corresponding mesh size and transferred into 50-mL pre-acid-washed falcon tubes. All of these had been prepared by acid wash and then deep rinsed with local seawater before sample collection. All samples were refrigerated during transport to Plymouth Marine Laboratory and then stored at  $-20^{\circ}\text{C}$  in the dark until processing.

#### *Sample processing and analysis*

*eDNA extraction, amplification, sequencing, and sequence analyses.*—A full description of the molecular methods employed can be found in Appendix S2. In brief, eDNA was extracted from sediment samples using the Qiagen Dneasy PowerSoil (Qiagen, Hilden, Germany) extraction kit following the manufacturer's guidelines. The V9 region of the 18S rRNA gene was amplified using Earthmicrobiome project 18S rRNA gene universal primer pair Euk1391F (GTACACACCGCCCGTC) and EukBr (TGATCCTTCTGCAGGTTACCTAC) (available online).<sup>9</sup> This primer pair is based on those first published by Amaral-Zettler et al. (2009) but has been subsequently modified to minimize amplification of bacteria and archaea. The pair was chosen as it is known to amplify a diverse range of seaweed sequences, including the focal species we targeted within this study. Sequencing was carried out using MiSeq by commercial contract (Mr DNA, Molecular Research LP, Shallowater, Texas, USA). Distinct Operational Taxonomic Units' sequences were then allocated to taxa at the lowest possible taxonomic resolution using the Basic Local Alignment Search Tool (BLAST) of the National Centre for Biotechnology Information (NCBI, U.S. National Library of Medicine), and then individually quality controlled. We report here on minimum percent homology, that is, the minimum match between a sampled sequence and a (set of) record (s) in the NCBI BLAST (SI), which can be used as a measure of confidence in the sequences reported in this study. The retrieved list of taxa was cross-referenced manually in the World Register of

<sup>8</sup> www.marinespecies.org

<sup>9</sup> www.earthmicrobiome.org

Marine Species (see footnote 8) to isolate macroalgae, verifying their habitat (only marine species were included) and taxonomic classification. Taxa sequenced only one time (i.e., only one sequence in all samples) were considered spurious sequencing results and excluded from subsequent analysis. The resulting DNA occurrence records for individual macroalgal taxa (lowest level possible) in L4 sediments was analysed in PRIMER 6.0 (v6.1.11; PRIMER-E Ltd, Plymouth, UK). Bray-Curtis similarity of the taxa sequence count by sample matrix was square-root transformed to down-weight common taxa in all analyses. Nonmetric multidimensional scaling (nMDS) plots were used to visualize key groupings among sampling dates reflecting similarity in the taxonomic composition of macroalgal DNA detritus in sediments. The statistical significance of differences among dates was tested using one-way analysis of similarity (ANOSIM), considering sampling date as the predictor and 999 permutations. Taxonomic differences between date groups were analysed using the similarity percentages routine (SIMPER).

*Analysis of  $\delta^{13}\text{C}$  in DIC samples.*—The stable isotope of carbon in  $\text{CO}_2$  gas released into the headspace of Exetainers containing the DIC water samples was analysed using a Gas-bench II connected to a DeltaPlus Advantage isotope ratio mass spectrometer (both Thermo Finnigan, Bremen, Germany; James Hutton Institute, Dundee, UK). The technique employed is detailed in Appendix S2. No  $\text{CO}_2$  intrusion was detected in control Exetainers, analysed in the same way.

*Carbon and nitrogen assimilated and buried by macrofauna.*—All phyto- and zooplankton, macrofauna, macroalgae, filters, and BSed samples were processed prior to elemental scans (C and N content) and stable isotope determination ( $\delta^{13}\text{C}$ ,  $\delta^{15}\text{N}$ ) of TPC, POC, and TPN. The processing method is detailed in Appendix S2.

Elemental analysis was undertaken using a constant flow isotope ratio mass spectrometer (Sercon model 20-20s, dual turbo pumped, CF/IRMS) connected to a Thermo EA1110 elemental analyzer, NC dual tube configured, with a high performance Carbosieve G separation column (OEA Labs, Callington, UK). The technique employed is detailed in Appendix S2.

*Carbon assimilated by meiofauna.*—The techniques employed to wash meiofauna samples are detailed in Appendix S2. All glassware and materials were briefly acid washed as before. From each sample, 100–120 picked nematodes that had been cleaned of sediment were placed in an oven-muffled ( $550^\circ\text{C}$ , overnight) aluminum cup ( $5.25 \times 3.2$  mm), which was filled with two drops of Milli-Q; for each cup, the number of nematodes was registered. These cups were then placed in a multi-well plate and oven-dried overnight at  $60^\circ\text{C}$ ; they were then crimp-closed in preparation for C elemental analysis. During each working session in the lab, a number

of control cups were run to assess laboratory contamination; these cups were treated in the same way as the sample cups but only contained two drops of Milli-Q. Elemental analysis of these control samples showed no C contamination. Prepared sample masses ranged between 7 and  $30 \mu\text{g C}$ , with an average of  $12 \mu\text{g C}$ . Elemental screening for POC and isotopic determination of  $\delta^{13}\text{C}$  was undertaken as for macrofaunal samples.

*Bayesian stable isotope mixing modeling.*—The package MixSiar (Stock and Semmens 2016a) for R (version 3.4.1; R Core Development Team, Vienna, Austria) was used to construct Bayesian Stable Isotope Mixing Models (SIMM) to partition the sources of organic matter used by macrofauna (and meiofauna), as well as that available within sediments, over the studied seasonal cycle. MixSIAR uses Markov chain Monte Carlo (MCMC) methods to estimate diet mixes, expressed as posterior probability distribution functions, based on a generalist prior and, in this case, bulk stable isotopes as biotracers (Stock and Semmens 2016a). This approach accounts for the variability in sources, as measured over the seasonal cycle, as well as unknown sources of error (appropriate for undetermined systems such as estuarine areas) and provides information about the uncertainty in diet mixes generated by each model (Parnell et al. 2013). We built separate models for macrofauna, meiofauna, and sediments (BSed), considering the following sources: SPOM at 70 cm above the sediment water interface (hereafter, SPOM70), phytoplankton, zooplankton, and macroalgal communities sampled at two shore sites; all aggregated per source and time point.

We built separate models for macrofauna within each sediment layer (0–2, 2–6, and 6–10 cm) to discriminate whether the influence of food sources was discernibly variable with sediment depth. Initial tests showed that this approach provided better MCMC convergence than constructing one single model for all macrofauna across the 10 cm deep core. All models for macrofauna were built using isotopic and elemental content referring to particulate organic carbon (POC) and total particulate nitrogen (TPN). The source input matrix contained the mean and standard deviation of the  $\delta^{13}\text{C}$  and  $\delta^{15}\text{N}$  of each source (over the seasonal cycle), their elemental concentration of biotracers (i.e., C and N); and data sample size. For the consumers (i.e., macrofauna), we included  $\delta^{13}\text{C}$  and  $\delta^{15}\text{N}$  data (non-aggregated over time). Sampling date was included in the three macrofaunal models as a continuous covariate, across which consumer data were allowed to vary, as well as a static covariance matrix independent of source covariance, improving previous Bayesian SIMM assumptions (Stock and Semmens 2016a). The latter choice was appropriate because the resulting diet mixes are likely to depend on unmeasured factors not linked to specialization of consumers regarding sources or discrete feeding events (Stock and Semmens 2016b). Rather, they likely reflect some or all of the following, as well as other factors:

variability in source abundance and natural hydrodynamic processes determining what and how much carbon from each potential source reaches the seabed, temporal variations in sediment conditions and the structure of the macrofaunal community, and variation in assimilation times across individual species. As local benthic macrofauna included a large proportion of suspension and deposit feeders (Appendix S1: Table S2) with various ecological strategies, we assumed that macrofauna, as the consumer in each of the three models, had direct access to any suspended particulate food resources near the seabed. In the absence of detailed dietary information for fauna at our study site, we included the widely used tissue discriminatory factors of 1‰ and 3‰ for C and N, respectively, for all sources (DeNiro and Epstein 1978, Wada et al. 1991, Phillips et al. 2014). These were later verified against the stable isotope determination results. The MCMC algorithm parameters employed were chain length = 100,000; burn in = 50,000; thin = 50; and chains = 3. MCMC convergence was assessed based on Gelman-Rubin diagnostic statistic and Geweke statistic calculations (Stock and Semmens 2016a).

The same procedure was used to build a Bayesian SIMM for meiofauna. Due to naturally low nitrogen content of meiofauna, this model was built based on  $\delta^{13}\text{C}$  and POC only (i.e., one stable isotope, instead of two). Due to the lower power of the resulting data set, we had to exclude concentration data as well as the time covariate in the meiofaunal model.

Initial tests for the model for sediments (BSed) indicated that sediment depth as a factor did not increase the convergence of the models, so we ran one single model for sediments. However, initial biplots indicated that sediment samples clearly separated along a  $\delta^{13}\text{C}$  gradient, with samples in March to September (summer) being enriched in  $^{13}\text{C}$  relative to those in the remaining months of the year (winter). In this model, we therefore expressed the effect of time on our system using this grouping as a fixed effect.

#### *Benthic-pelagic process measurements: burial, sediment flushing, and carbon mineralization*

Processes involved in non-trophic sedimentary carbon uptake (sediment flushing and burial) and loss (respiration) were investigated. To this end, during each Station L4 sampling trip, and from paired squared cores retrieved from box core deployments, one core (~20 cm deep) and the water overlying the sediment were collected using an acrylic aquarium that had its bottom cut off. This core was immediately sealed using a PVC shoe fitted with a rubber and neoprene seal and was used for bioturbation incubations (hereafter, bioturbation cores). The second squared core from each box core (~20 cm) was collected and transferred into a same-sized squared aquarium using the method in Queirós et al. (2014), and a profiling  $\text{O}_2$  optode sensor array mounted to it

(OxyMini, World Precision Instruments, similarly to Queirós et al. [2014]). This second core was used for respiration and bioirrigation incubations (hereafter, bioirrigation cores).  $\text{O}_2$  optode sensors were calibrated prior to each sampling date, following the manufacturer two-point calibration protocol, and using 100% dissolved-oxygen-saturated seawater and Zero Oxygen Solution (Hannah Instruments, Woonsocket, RI, USA). All aquaria were gently topped up using local seawater on deck, and were individually aerated using diffusing air stones and shaded during the 4–6 h transport to the PML mesocosm laboratory. This is a temperature-controlled room where the air temperature is regulated on a monthly basis so that aquaria in the room follow the seasonal temperature cycle of bottom seawater at Station L4 (Findlay et al. 2008, Queirós et al. 2015a). On arrival to the mesocosm laboratory, the temperature of seawater overlying each core was recorded again, verifying that it had not risen by more than 2°C. All cores were then connected to a recirculating water system, supplied using peristaltic pumps (~20 mL/min) from a 1-m<sup>3</sup> batch of filtered seawater (10  $\mu\text{m}$  and 1  $\mu\text{m}$  hydrex block carbon filters). This water had been collected at L4 on the week prior to each benthic sampling date; it was continuously aerated using diffusing air stones and kept in the dark to prevent autotroph growth.

*Carbon mineralization and bioirrigation incubations.*—Geochemical profiles and fauna in the bioirrigation cores were allowed to resettle overnight in the laboratory. The following morning, each core was disconnected from the recirculating water system and covered by a lid onto which a motorized vane had been fitted, continuously and gently stirring the water at 5 rpm, without causing resuspension. Respiration and bioirrigation incubations were initiated using the protocol that follows, for each core. These incubations were undertaken primarily to investigate potential changes in bioirrigation rates (i.e., exchange of fluid between sediment and water column, hereafter, sediment flushing) and total oxygen uptake (TOU, i.e., benthic community respiration).

Sodium bromide (NaBr) was used as an inert tracer to estimate bioirrigation rates (Forster et al. 1999). A pre-weighed amount of NaBr was mixed with core water and added to each aquarium to achieve a molarity of 10 mmol/L, given the measured water volume in each full aquarium. At this stage, the dissolved oxygen concentration was measured at the sediment water interface (0–0.5 cm deep) using the profiling  $\text{O}_2$  optode array (see Queirós et al. 2014 for setup and measurement rate). The motorized vane was then turned on and flow initiated. A 10-mL water sample was collected 15 min after tracer addition to determine the initial Br concentration, using sterile syringes and falcon tubes that had been pre-rinsed with 5 mL of this water twice. Each aquarium's lid was then sealed using biological grade silicon sealant (Gold Label, Hotton Aquatic Products, Dorset, UK)

and the cores left to incubate in the dark for 4 h. At the end of this period, dissolved oxygen readings were taken again using the optode system, followed by opening of cores to collect a second Br sample, as before. Samples were stored frozen at  $-20^{\circ}\text{C}$  until analysis. Bioirrigation rates ( $\text{L}\cdot\text{m}^{-2}\cdot\text{d}^{-1}$ ) were determined from the decrease in bromide concentration in the water column between the beginning and the end of incubations, indicating the net volume of water entering the seafloor (Forster et al. 1999). Bromide concentrations were determined using reversed-phase high performance liquid chromatography (HPLC; Gazeau et al. 2014) using the technique detailed in Appendix S2. The bioirrigation rate estimated in these cores at each time point (sediment flushing,  $\text{L}\cdot\text{m}^{-2}\cdot\text{d}^{-1}$ ) was then multiplied by the average concentration of suspended POC measured in the water sampled from multi-cores in the field on the same occasion (average of measurements at 0 and 70 cm above the seabed), derived via elemental analysis of SPOM filter samples and the volume of water filtered on deck to acquire these samples (POC g/L). This calculation therefore quantified the impact of faunal-mediated sediment flushing on the sedimentary uptake of POC ( $\text{mol}\cdot\text{m}^{-2}\cdot\text{d}^{-1}$ ), at each time point.

Total oxygen uptake was determined from the change in dissolved oxygen measured during the incubations using the sediment-water interface optode sensor spot. Optode readings (percent dissolved oxygen) were converted into oxygen concentration considering the effects of temperature and salinity on dissolved oxygen saturation, according to Weiss (1970). The amount of  $\text{CO}_2$  respired (i.e., mineralized, DIC production,  $\text{mol}\cdot\text{m}^{-2}\cdot\text{d}^{-1}$ ) was approximated from these values via the widely used respiration stoichiometry of 1:1, and a respiration coefficient of 0.85, which accounts for an average, potential uptake of oxygen by inorganic processes (Glud 2008).

*Burial of carbon via bioturbation.*—On the day following the bioirrigation assessments, bioturbation incubations were initiated using the methods detailed in Queirós et al. (2015b). Briefly, we used fluorescent particle tracing (Mahaut and Graf 1987) within a UV time-lapse photography setup (Schiffers et al. 2011) to measure faunal sediment reworking activity within bioturbation cores, over seven days (hereafter, bioturbation). Orange luminophores were used as a fluorescent particle tracer (Appendix S1: Fig. S2), which had been custom made by Partrac Ltd (Heatfield, UK) to match the sediment granulometry at the benthic site of Station L4. The tracer serves as a proxy for particulate material deposited at the surface of the sediment, and its net transport below the sediment surface, at the end of the incubations, therefore approximates net sediment burial rates driven by macrofauna bioturbation. The resulting net transport of sediment below the sediment surface was estimated as [100% – percentage of tracer left at the initial tracer layer depth] at the end of the incubation (%/

d). For each sampling occasion, this rate was multiplied by the average estimated POC available at the same sediment depth, based on the POC content measured in the surficial sediment layer in the field (0–2 cm) via elemental analysis of BSed samples ( $\text{POC mol}/\text{m}^3$ ). This calculation was then used to quantify the impact of bioturbation on the rate of burial of POC below the sediment surface ( $\text{mol}\cdot\text{m}^{-2}\cdot\text{d}^{-1}$ ), at each time point. This value was added to the estimated rate of POC flushing via bioirrigation to estimate a minimum rate of POC uptake rate in sediments, based on these faunal-mediated processes. The proportion of this POC flux associated with material of macroalgal origin was estimated based on the corresponding use of macroalgal detritus in faunal diets, estimated from the BSIMMs.

*Net carbon sequestration estimates.*—The two types benthic-pelagic processes measured (uptake and mineralization) are mediated by seabed communities and contribute to determining the fate of organic carbon available to the seabed (Snelgrove et al. 2018). We used these measurements to inform the potential for sediments to serve as a blue carbon sink, both in terms of the macroalgae detritus and overall POC storage. At each sampling point, we then estimated a theoretical minimum carbon sequestration: (1) assuming that DIC production was entirely fueled by mineralization of POC that entered the seabed and (2) considering the proportion of net POC sequestered within the seabed via those mechanisms that had macroalgal origin. We estimated 1 as the total POC uptake mediated by fauna (via bioturbation and bioirrigation) minus the DIC produced. We estimated 2 by multiplying the average contribution of macroalgae to macro- and meiofauna diets by 1, given that these are the organisms mediating the benthic-pelagic uptake processes we measured. Additional processes contributing to uptake, such as sedimentation, would be expected to increase net sequestration.

## RESULTS

### *Shore surveys: macroalgal detritus loss*

A high relative proportion of young individuals of two of our four focal macroalgal species (*F. serratus* and *H. elongata*) was found at both shores during autumn and winter, reflecting the large seasonal loss of reproductive biomass and post-reproductive fronds to coastal waters (Knight 1947, Moss 1969). This effect was particularly evident during sampling between September 2015 and January 2016. Well-developed reproductive fronds were observed again on surveyed shores from March 2016. Two other shore species were sampled: *L. hyperborea* and *S. latissima*. They are largely abundant in biomass locally (UK Archive for Marine Species and Habitats Data), being pseudoperennials (long-lived and short-lived, respectively) with continued loss of small, distal detritus throughout the year, accentuated by loss

of whole, old blades between spring and autumn (Parke 1948, Lüning 1971, Sjøtun 1995). Loss of whole individuals (with stipe) is also known to occur during large storms, from late summer and through winter, leading to conspicuous beach stranding of whole individuals of both species (Smale and Vance 2015; Queiros, *personal observation*).

#### *Macroalgal detritus in L4 sediments*

eDNA corresponding to 148 distinct macroalgal taxa belonging to 34 orders of red, green, and brown algae, were identified within the sediment at Station L4 (Appendix S1: Table S1). Minimum percent homology reported in the table provides a measure of confidence in each of the sequences reported (“match”) and the sources and quality of NCBI sequences used within this supplementary table were carefully checked to ensure they were genuinely macroalgal DNA sequences. eDNA from all except two out of 16 orders of macroalgae previously reported in the region (UK Archive for Marine Species and Habitats Data) occurred within sediments, at least at some time during the year. Focusing on species sampled on the shore, all sequences identified as *Laminaria* spp., *Saccharina* spp., *Fucus* spp., and *Himantalia* spp. were aligned against those found within the NCBI database (Fig. 2a). *F. serratus* was found only between January and May and *H. elongata* was not found during autumn (Appendix S1: Table S1). The fragment of the 18S rRNA gene utilized in this study is not sufficient to differentiate between the Laminariaceae *L. hyperborea* and *S. latissima*, which are grouped closely based on likelihood and bootstrap analyses (Fig. 2a). Sequences grouping with these Laminariaceae could be detected throughout the year, as would be expected based on the local phenology of these two species (Fig. 2a, Appendix S1: Table S1). Overall, the taxonomic composition of macroalgal eDNA in sediments varied significantly between sampling dates (Fig. 2b, ANOSIM Global  $R = 0.335$ ,  $P < 0.001$ ). Early year samples (January and March) were the most dissimilar from all others and from each other (ANOSIM pairwise tests using date as grouping,  $P < 0.005$ ), and November exhibited intermediate composition between this group and all other samples. Sediment samples from May–September 2015 and May 2016 were similar in macroalgal DNA composition (ANOSIM pairwise tests using date as grouping,  $P > 0.05$ ).

#### *Isotopic tracing of sources of organic carbon entering the benthic system*

*Seasonal variation in environmental conditions and organic matter pools.*—Tracing organic matter using stable isotopes, from sources to potential sedimentary sinks, requires an understanding of how these signals may themselves vary at sources (Parnell et al. 2013). The water column conditions at Station L4 exhibited marked

seasonality (Fig. 3), which was apparent in the stable isotope of dissolved inorganic carbon in bottom waters (DIC, Fig. 3a). Bottom seawater was enriched in  $^{13}\text{C}$  in spring and summer compared to winter, with  $\delta^{13}\text{C}$  decreasing by as much as 4.40‰ (and 5.21‰) 70 cm above (and at) the sediment–water interface. This pattern could be seen to suggest net autotrophy at L4 during the growing season in spring and summer months (Fig. 3a), during which light C isotopes are preferentially taken up by primary producers, enriching the  $\delta^{13}\text{C}$  of DIC (Fry 2007). However, the light attenuation coefficient at the site rules out this hypothesis: <1% of light reaches the 48 m deep seabed (Appendix S1: Fig. S3), suggesting instead that primary produced organic matter arriving at L4 is allochthonous (as noted by Tait et al. 2015). Seasonal variations of  $\delta^{13}\text{C}$  of bottom water DIC at L4 are consequently interpreted as more likely to reflect intense photosynthetic activity in surface waters during the spring and into autumn and seasonal diversity in the mechanisms of organic matter degradation and availability near the seabed.

The elemental content and stable isotope characterization of all sources used in our Bayesian SIMMs (Table 1a; two macroalgae communities, SPOM at 70 cm above the seabed, and phyto- and zooplankton) highlight seasonal variability in  $\delta^{13}\text{C}$  as well as  $\delta^{15}\text{N}$  in these POC and TPN pools. This variability was included as the standard deviation around the mean in the source input matrix used in all Bayesian SIMMs. These estimates (Table 1a) follow the general expectation of a gradient of increased depletion in  $\delta^{13}\text{C}$  of resources, from nearshore to offshore (Miller and Page 2012). Indeed, we found a good separation between planktonic (offshore) and macroalgal (onshore) communities, supporting their use as distinct sources of organic matter in our Bayesian SIMMs, and overcoming some of the difficulties challenging previous work (Hill et al. 2015). Differences in the stable isotope signatures of phyto- and zooplankton corroborate the expected trophic enrichment factor of 1‰ and 3‰ for  $\delta^{13}\text{C}$  and  $\delta^{15}\text{N}$  (Table 1a), and indicate that our sampling strategy for these pools was also adequate. We used these factors in our Bayesian SIMMs. POC and TPN content for all sources were also calculated and used in the Bayesian SIMMs (Table 1a). Their concentration relative to seawater volume was additionally calculated for phyto- and zooplankton (assuming maximum net efficiencies of 95%), and SPOM70 (Table 1a).

The two macroalgal communities sampled were sufficiently isotopically distinct over the seasonal cycle to justify their separation as separate sources in the Bayesian SIMMs (Table 1a). However, we were not able to consider as many sources due to model power constraints. Initial modeling tests indicated that macroalgae from Rame Head had a higher probable contribution to macrofaunal diets than those from Plymouth Hoe (Fig. 1), with detritus release from the former therefore more likely to represent a route of connectivity between

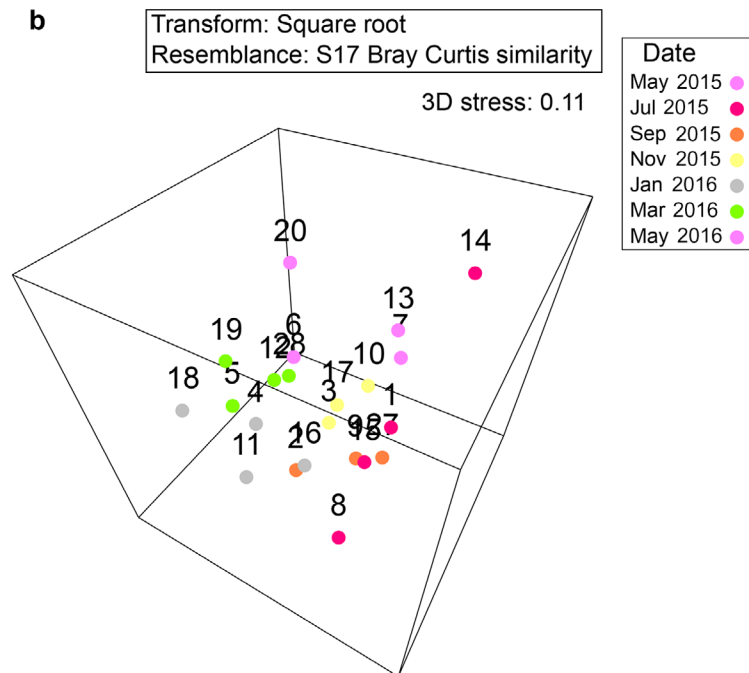
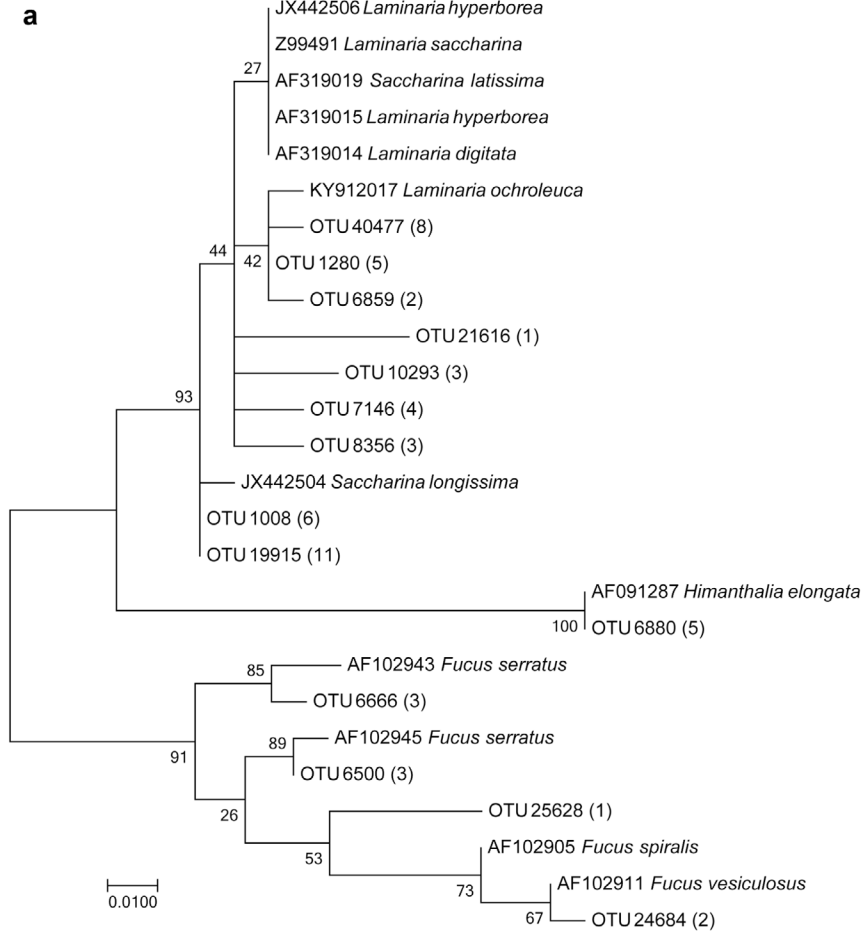


FIG. 2. Macroalgal species identified in L4 sediments using eDNA sequencing. (a) The 18S rRNA gene sequences identified as a close match to our four focal species, alongside previously reported sequences and their accession numbers. The number of sequences clustered within each OTU is shown in parentheses. The tree topology is based on maximum likelihood and bootstrap analysis was performed with 1,000 replications (MEGA5). (b) Nonmetric multidimensional scaling (NMDS) plot illustrates the Bray-Curtis similarity of sediment samples, considering individual macroalgal taxon sequence counts, with colors identifying the sampling date and numbers identifying individual sediment samples.

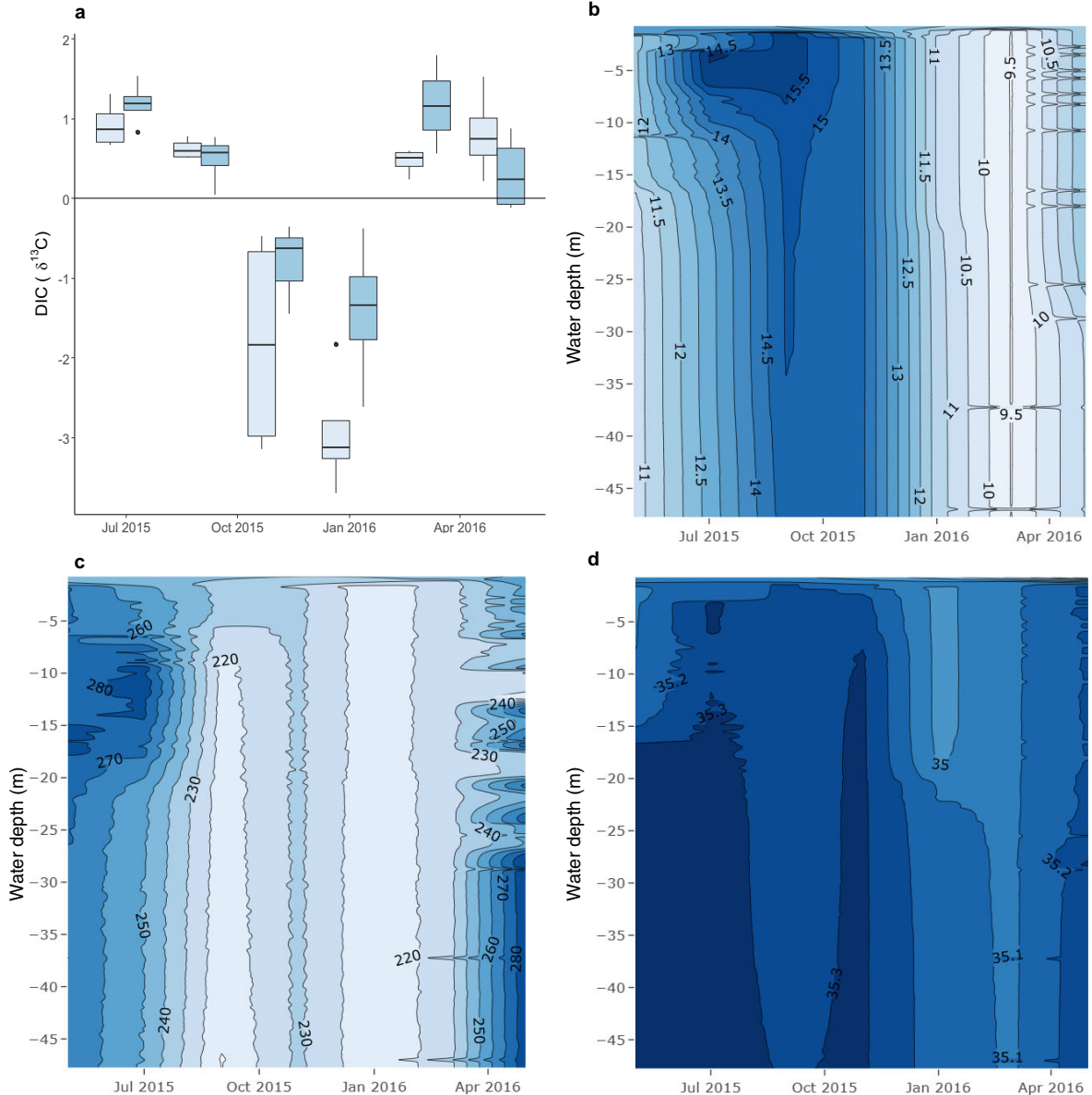


FIG. 3. Seasonal cycle of environmental conditions at Station L4, relative to sampling date, as measured using multi-corer samples (a, benthic site) and CTD profiles (b–d, main site). (a) Carbon stable isotope of dissolved inorganic carbon (DIC) in seawater near the seabed at Station L4’s benthic site. Measurements were undertaken in bottom water (0 cm, light blue), and 70 cm above the seafloor (dark blue). Box plot components are mid line, median; box edges represent the 1st and 3rd quartiles; whiskers represent the maximum and minimum; and dots are maximum or minimum when less than four samples were available. (b) Contours give seawater temperature (°C) depth profiles (yy, y-axis; m, meters). (c) Contours give dissolved oxygen molarity depth profiles (yy, y-axis; m, meters). (d) Contours give seawater salinity (PSU) depth profiles (yy, y-axis; m, meters).

TABLE 1. Elemental content (percent dry mass, %), concentration (mg/L water column seawater/sediment), and stable isotope composition (‰) of particulate organic carbon (POC) and total particulate nitrogen (TPN) of different pools, as measured over the seasonal cycle (mean ± SD).

Location	Pool	Depth (m)	$\delta^{13}\text{C}$ (‰)	$\delta^{15}\text{N}$ (‰)	POC (‰)	POC (mg/L)	TPN (%)	TPN (mg/L)	n
a)	Hoe	0–1	-15.48 ± 1.79	7.66 ± 1.45	28.06 ± 3.68	NA	2.28 ± 0.53	NA	30
	Rame	0–1	-17.04 ± 1.61	7.21 ± 0.62	28.98 ± 3.65	NA	1.78 ± 0.55	NA	21
	L4	0–20	-20.71 ± 1.98	6.31 ± 2.20	0.32 ± 0.22	$1.16 \times 10^{-3} \pm 0.84 \times 10^{-3}$	0.04 ± 0.03	$0.17 \times 10^{-3} \pm 0.09 \times 10^{-3}$	6
	L4	0–48	-19.77 ± 1.50	9.09 ± 2.79	5.48 ± 3.91	$1.07 \times 10^{-3} \pm 1.44 \times 10^{-3}$	1.44 ± 0.99	$0.29 \times 10^{-3} \pm 0.38 \times 10^{-3}$	6
	L4	47.3	-22.58 ± 1.02	4.09 ± 2.25	0.35 ± 0.11	1.92 ± 1.55	0.04 ± 0.02	0.17 ± 0.16	14
	b)	L4	47.9	-21.22 ± 0.53	4.36 ± 2.94	0.45 ± 0.11	6.92 ± 4.91	0.04 ± 0.02	7.16 ± 24.71
L4		48	-19.76 ± 0.90	4.40 ± 0.35	0.21 ± 0.03	2.54 ± 0.76	0.03 ± 0.01	0.41 ± 0.14	28
L4		48	-20.04 ± 0.82	4.59 ± 0.17	0.25 ± 0.04	3.29 ± 1.06	0.04 ± 0.01	0.55 ± 0.13	28
L4		48	-19.76 ± 1.53	4.62 ± 0.16	0.25 ± 0.02	3.34 ± 0.68	0.04 ± 0.00	0.56 ± 0.10	28
L4		48	-19.76 ± 1.53	4.62 ± 0.16	0.25 ± 0.02	3.34 ± 0.68	0.04 ± 0.00	0.56 ± 0.10	28
L4		48	-19.76 ± 1.53	4.62 ± 0.16	0.25 ± 0.02	3.34 ± 0.68	0.04 ± 0.00	0.56 ± 0.10	28

Notes: The number of samples used is n. (a) Organic matter pools considered as sources in Bayesian Stable Isotope Mixing Models. Plankton samples from March 2016 were lost during processing. (b) Sediments at the benthic site of Station L4. Locations per Fig. 1 (Hoe is Plymouth Hoe; L4 is Station L4 in a, and the benthic site in b; Rame is Rame Head). Values are means ± SD. NA, Not available.

shore macroalgae and L4 sediments than the latter. The final Bayesian SIMM estimates therefore include data from the Rame Head macroalgal community only, not both communities.

The elemental content and isotopic characterization of L4 sediments and fluff layer indicate that the  $\delta^{13}\text{C}$  of POC did not vary markedly with sediment depth, though  $\delta^{15}\text{N}$  exhibited  $^{15}\text{N}$  enrichment with depth (Table 1b). Considering the average marine sediment wet bulk density of 1.7 kg/L (Tenzer and Gladkikh 2014), we also scaled POC and TPN content measurements per unit of volume of sediment (wet mass, Table 1b). The seasonal variability of POC content with depth, from 70 cm above the sediment water interface to 10 cm within the sediment (mg/L) could then be calculated (Appendix S1: Fig. S4). POC content generally increased along this depth profile, and peaked in May and September months, potentially reflecting both plankton blooms as well as the loss to detritus from several macroalgal species along the shores (Parke 1948, Lüning 1971, Sjøtun 1995, Tait et al. 2015).

*Sources of organic matter assimilated by sedimentary macrofauna.*—Biplots, illustrating the stable isotopic signatures of macrofauna at 0–2, 2–6, and 6–10 cm relative to the studied sources (phyto- and zooplankton, macroalgae, and SPOM; Fig. 4a–c), indicate that the  $\delta^{13}\text{C}$  ranges of organic carbon in macrofauna occur well within the ranges of sampled sources. Zooplankton has a higher  $\delta^{15}\text{N}$  range than benthic invertebrates, and this may reflect the proportion of higher trophic level species (e.g., fish larvae) in the community at certain times of year (Reygondeau et al. 2015).

The corresponding Bayesian SIMMs (Fig. 4d–i) exhibited convergence, with a Gelman-Rubin diagnostic within the range [1, 1.05] and the Geweke statistic within [-2, 2] (Stock and Semmens 2016a). The correlation between the isotopic signature of SPOM and each of the other sources considered in the Bayesian SIMMs (phyto- and zooplankton, and macroalgae Appendix S1: Fig. S5) indicates that organic matter of origin other than these explicit sources (i.e., diffuse origin and potentially including terrestrial material) was an important part of this pool, as expected in this relatively near shore environment (Smyth et al. 2015).

Each source’s estimated contribution to macrofaunal diets is not an instantaneous snapshot, but rather a reflection of assimilation over time, so some lag could occur between the maximum uptake of a given food source and a change in a consumer characterization (Middelburg 2014). The posterior probability distributions indicating diet partitions for macrofauna at different sediment depths were estimated in two ways: aggregated over the seasonal cycle (Fig. 4d–f), and partitioned over time (Fig. 4g–i). For fauna at the sediment surface (Fig. 4d), each food source contributes about one-quarter of the seasonally aggregated diet (macroalgae,  $21.2\% \pm 18.2\%$ ; phytoplankton,  $28.3\% \pm 20.1\%$ ;

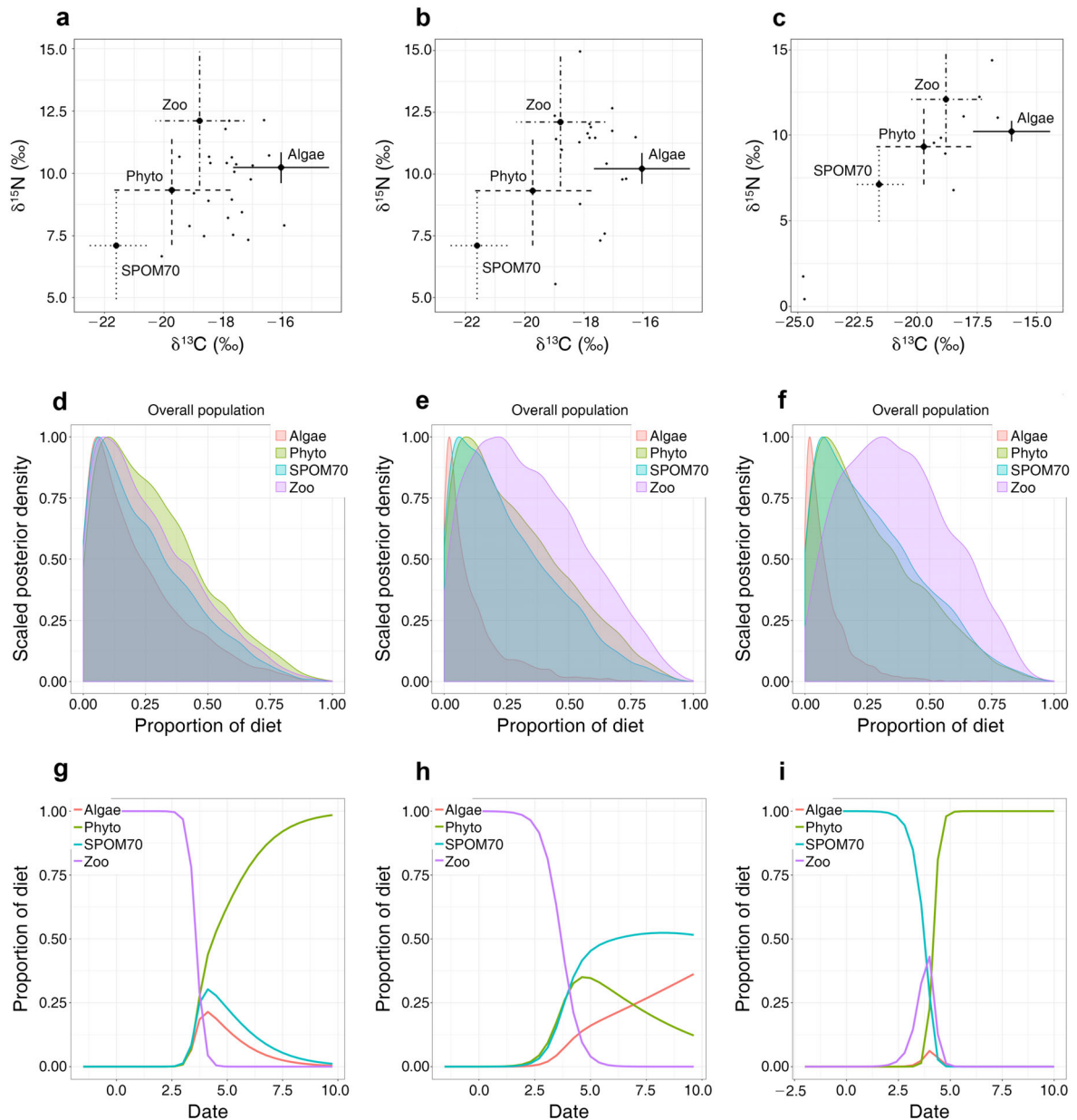


FIG. 4. Bayesian stable isotope mixing modeling results for macrofauna. Sources are phyto- and zooplankton (Phyto and Zoo), macroalgae (Algae), and suspended particulate organic matter from 70 cm above the sediment surface at the coastal site (SPOM70). (a–c) Biplots showing the stable isotope signatures of sources and macrofauna over the seasonal cycle (a, 0–2 cm; b, 2–6 cm; and c, 6–10 cm). (d–f) Posterior probability distributions for each source's contribution to macrofauna diets when all sampling dates were combined (d, 0–2 cm; e, 2–6 cm; and f, 6–10 cm). (g–i) Posterior probability distributions for each source's contribution to macrofauna diets relative to sampling date (g, 0–2 cm; h, 2–6 cm; I, 6–10 cm). There were seven sampling dates, two months apart, with date 1 = May 2015; date 7 = May 2016.

zooplankton,  $26.3\% \pm 19.7\%$ ; SPOM70,  $24.3\% \pm 19.1\%$  [mean  $\pm$  SD]. Two patterns emerge as the distance to the sediment–water interface increases (2–6 cm and 6–10 cm sediment layers, Fig. 4e, f): (1) the uptake of macroalgae and phytoplankton in diets decreases and (2) the uptake of zooplankton material and SPOM70 increases. Consequently, at 6–10 cm depth in the

sediment, diets are strongly dominated by zooplankton material and seaweeds contribute very little (macroalgae,  $8.6\% \pm 9.5\%$ ; phytoplankton,  $26.5\% \pm 20.1\%$ ; zooplankton,  $37.5\% \pm 20.7\%$ ; SPOM70,  $27.4\% \pm 20.2\%$ ). The large variability observed in these seasonally aggregated posterior probability distributions reflects the marked seasonality of macrofaunal diet

partitioning, across the different sediment depths (Fig. 4g–i, seven sampling occasions starting in May 2015 and ending in May 2016). At the surface (Fig. 4g), diets are dominated by zooplankton from early summer and into autumn; macroalgae and SPOM70 are important during winter; and phytoplankton dominates from the onset of the spring bloom. At 2–6 cm (Fig. 4h), zooplankton still dominates diets in the same period as at the surface, but diet proportions change for the other food sources, with SPOM70 becoming a more important resource from the autumn onward. At 6–10 cm (Fig. 4i), SPOM70 dominates diets from early summer and into autumn, with a peak in the zooplankton contribution (and to a very small extent, that of macroalgae) during the autumn bloom, and phytoplankton dominates again from the onset of the spring bloom.

*Sources of organic matter assimilated by meiofauna.*—The Bayesian SIMM used to estimate meiofaunal diet apportionment (Fig. 5) exhibited convergence, with Gelman-Rubin diagnostic within the range [1, 1.05] and the Geweke statistic within [−2, 2] (Stock and Semmens 2016a). Given that the seasonal cycle is aggregated in this model (no time covariate), the posterior probability distributions of meiofaunal diet contributions suggest that zooplankton and macroalgae are the most important food sources (macroalgae,  $36.3\% \pm 14.1\%$ ; zooplankton,  $26.6\% \pm 19.5\%$ ), above phytoplankton and SPOM70 (phytoplankton,  $22.7\% \pm 16.9\%$ ; SPOM70,  $14.3\% \pm 19.5\%$ ).

*Sources of organic matter found in L4 sediments.*—The Bayesian SIMM for sediments, with sedimentary stable isotopic signatures relative to studied sources, shows a clear temporal progression in sedimentary POC signatures (Fig. 6a). This pool exhibited enriched  $\delta^{13}\text{C}$  values

during spring and summer, becoming more depleted in  $^{13}\text{C}$  through the end of summer and into winter. This variation seemed to reflect primarily a loading of the system with zooplankton material during spring and summer (Fig. 6b), when this source contributed  $84.0\% \pm 24.6\%$  of organic matter in sediments. Tighter links between sediment and SPOM were measured during winter months (Fig. 6c, SPOM70 contributed  $90.3\% \pm 8.1\%$  to this organic matter pool). Other studied sources, including seaweed detritus, appeared to have a smaller direct contribution to the organic matter in L4 sediments, throughout the year. The corresponding Bayesian SIMM illustrated (Fig. 6b–c) exhibited convergence, with Gelman-Rubin diagnostic within the range [1, 1.05] and the Geweke statistic within [−2, 2] (Stock and Semmens 2016a).

#### *Net sequestration of POC at the seabed: blue carbon fluxes*

We estimated the minimum net POC sequestration, and net macroalgal organic carbon sequestration within the seabed (Fig. 7). Throughout the seasonal cycle (Fig. 7a), both fluxes were positive with the exception of January 2016, when POC uptake was very low. POC uptake peaked in May, leading to a net POC sequestration of  $12.87 \text{ mol}\cdot\text{m}^{-2}\cdot\text{yr}^{-1}$  in 2015 (and  $10.92 \text{ mol}\cdot\text{m}^{-2}\cdot\text{yr}^{-1}$  in May 2016, Fig. 7a). The corresponding peaks in net sequestration of macroalgal organic carbon at L4 sediments were  $1.92 \text{ mol}\cdot\text{m}^{-2}\cdot\text{yr}^{-1}$  in 2015 (and  $1.63 \text{ mol}\cdot\text{m}^{-2}\cdot\text{yr}^{-1}$  in May 2016, Fig. 7a). May was also the month when POC availability on the seabed was highest (Appendix S1: Fig. S4). Both fluxes exhibited marked seasonality in magnitude, as expected. The estimated annual average net blue carbon sequestration was  $4.89 \pm 5.50 \text{ mol}\cdot\text{m}^{-2}\cdot\text{yr}^{-1}$ , and the annual average net

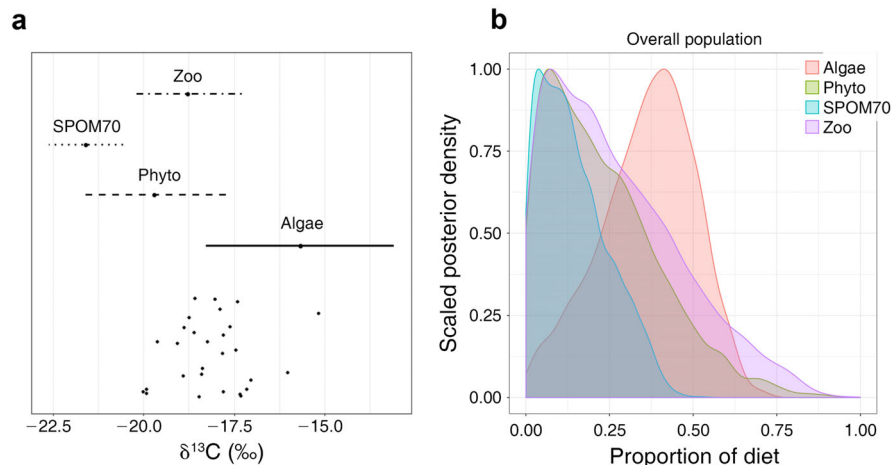


FIG. 5. Bayesian stable isotope mixing model results for meiofauna. Sources are phyto- and zooplankton (Phyto and Zoo), Rame Head shore macroalgae (Algae), and suspended particulate organic matter from 70 cm above the sediment (SPOM70). (a) Biplot showing the stable isotope signatures of sources and meiofauna (dots; 0–2 cm sediment), over the seasonal cycle. (b) Posterior probability distributions for meiofauna diet contributions of each source, when all sampling dates were combined.

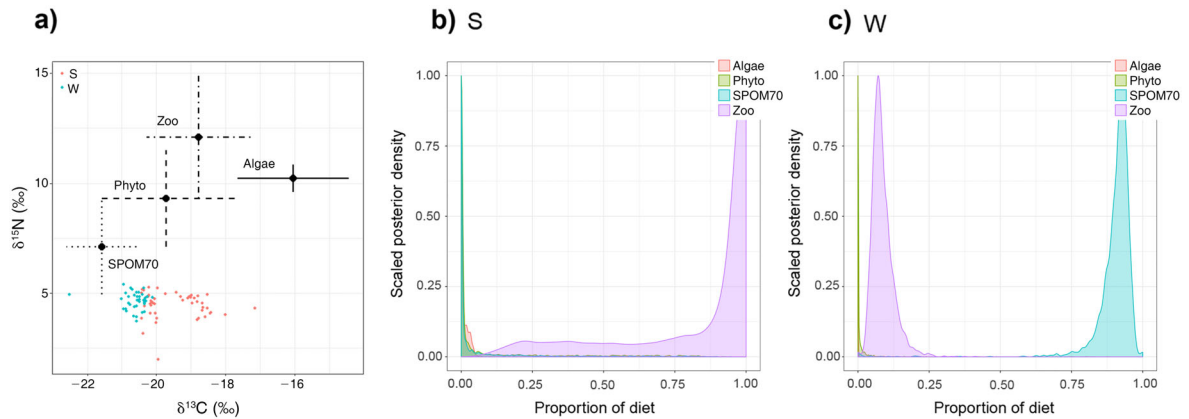


FIG. 6. Bayesian stable isotope mixing model results for organic matter in sediments at L4 (0–10 cm). Sources are phyto- and zooplankton (Phyto and Zoo), macroalgae (Algae), and suspended particulate organic matter from 70 cm above the sediment surface (SPOM70). (a) Biplots showing the stable isotope signatures of sources and sediments over the seasonal cycle, with s denoting samples collected in the months between March and September, and w denoting samples in November to January. (b and c) Posterior probability distributions for each source's contribution to sedimentary organic matter in March to September and November to January, respectively.

sequestration of macroalgal blue carbon was  $0.73 \pm 0.82 \text{ mol}\cdot\text{m}^{-2}\cdot\text{yr}^{-1}$  (Fig. 7b) at the site.

## DISCUSSION

Here, we have gathered important evidence that supports the view that connectivity between shore macroalgae and distal coastal sediments has a key food web role, and that it should be considered within blue carbon schemes (Hill et al. 2015, Smale et al. 2018). Specifically, using three lines of evidence (Bayesian SIMMs, eDNA, and process measurements) we demonstrated that macroalgal detritus, along with POC of different origins, enters the benthos of the coastal deep ocean and its food web, supporting a net positive carbon flux into the seabed annually. As predicted by others, we found this flux to occur throughout most of the year, unlike in other blue carbon habitats (Hill et al. 2015). Its magnitude is, however, markedly seasonal, reflecting processes intrinsic to the macroalgal community, as well as those driving detritus transport between donor shores and sink sediments. Focusing on a subset of the processes contributing to detritus uptake by the seabed, we highlighted that this flux exceeds mineralization rates most of the year, and should contribute to an annual growth of sedimentary carbon stores. Additionally, we found that it is not only the microbial loop that determines the fate of macroalgal detritus in sediments, as previously suggested (Rieper-Kirchner 1990). Rather, trophic and non-trophic processes mediated by seabed fauna make important contributions to the associated carbon fluxes, as highlighted in a recent global study (Snelgrove et al. 2018). Accounting for these contributions under blue carbon schemes will still require further data refinement via field measurements and transport model development. This study supports the view, however, that there

is no reason to continue to ignore that carbon leakage from macroalgae habitats is a fundamental transport pathway involved in the global blue carbon capacity of the ocean, supporting the growth of receiving sinks on the seabed (Duarte et al. 2013, Hill et al. 2015, Krause-Jensen and Duarte 2016, Krause-Jensen et al. 2018). These sinks also occur in the deep coast.

### *Macroalgal detritus enters the seafloor of the coastal ocean*

Studies that previously found macroalgal detritus to be an important organic carbon resource to coastal benthic communities (Polis et al. 1997, Krumhansl and Scheibling 2012) have at times been questioned given challenges in the sampling design and techniques employed in natural settings (reviewed by Miller and Page 2012). Taking these views into account, we deployed a robust sampling design and an array of complementary analytical approaches to overcome limitations. For instance, we used eDNA sequencing and bulk stable isotope analysis as complementary biotracing techniques (Nielsen et al. 2018), and both approaches indicated that macroalgal detritus enters deep coastal sediments. eDNA in sediments was indeed composed of that of many locally occurring macroalgal taxa, and the degree of match between each identified taxon and existing sequences within BLAST determines the confidence that can be placed in the origin of each material. The analysis of these data allowed us to achieve a high taxonomic discrimination of detritus, and thus to further identify how the regime of supply can be linked to the seasonal life-history processes of macroalgae. Specifically, detritus supply occurred year round, and the composition of macroalgal DNA in sediments varied through the year. The analysis of focal species allowed

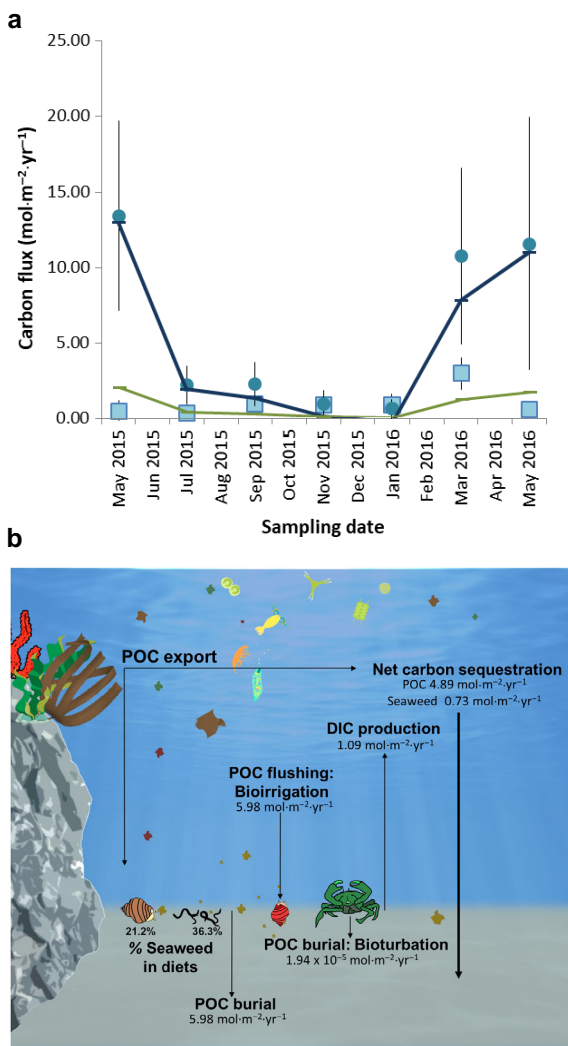


FIG. 7. The connected macroalgal–sediment system at Station L4. (a) Seasonal variability of biologically mediated processes influencing net POC sequestration at the seafloor, according to the availability of particulate organic carbon (POC) at the sediment near the seabed (Appendix S1: Fig. S4). Circles show total POC uptake (bioturbation and bioirrigation); squares show dissolved inorganic carbon (DIC) production; blue line shows blue carbon sequestration (total); green line shows seaweed blue carbon sequestration. (b) Seasonally averaged C fluxes and contributions to faunal diets.

us to link these patterns to species-specific patterns of detritus export, as had been documented for kelp (Filbee-Dexter et al. 2018). The lag times we observed between primary release periods and eDNA in sediments (*H. elongata* and *F. serratus*) potentially reflects different characteristics in the transport of the detritus exported between shore and sink. These could have included different surface cf. water column transport times, degradation rates, and amount of detritus produced relative to the overall eDNA pool, among other aspects. The connectivity between macroalgae and

sedimentary systems is thus not driven by physical processes alone (e.g., transport via currents and waves, gravitational detritus sedimentation). Furthermore, macroalgal detritus reaching coastal seabeds may not necessarily originate in proximate shores, drifting along- and offshore, covering considerable time and distance (Filbee-Dexter and Scheibling 2016). Despite this dynamic nature of the coastal ocean, it has been suggested that a large fraction of macroalgal detritus can still be retained coastally (Krause-Jensen and Duarte 2016, Smale et al. 2018). Our findings support this perspective, with our benthic study site located 13 km from the shore of Plymouth, at 48 m depth.

Net macroalgal carbon sequestration estimates were positive throughout, with the exception of one sampling occasion (January 2016) when POC supply to the seabed was very low. Although we did not age the carbon of our sediments, and thus cannot ubiquitously ascertain the residence time of this material within sediments, the three lines of evidence we pursued do suggest that macroalgal detritus contributes to net growth of coastal sedimentary POC stores. We did not choose this sedimentary site with prior knowledge of this connectivity and it is therefore likely that many other similar regions of the coastal ocean may retain macroalgal detritus (and carbon), outside of systems more frequently identified as blue carbon habitats (mangroves, seagrass beds and salt marshes). Identifying the location of hotspots for this sequestration will be an important step toward the inclusion of connected macroalgal-sediment systems within blue carbon management actions aimed at climate change mitigation.

#### *Macroalgal detritus: a resource to distal coastal benthic food webs*

Macrofauna and meiofauna at the surface of sediments are ideally placed to uptake food resources available in bottom waters. Macroalgae appeared to be an organic matter source preferentially assimilated by both groups (cf. Rieper-Kirchner 1990, Hill et al. 2015), as found in other systems (Renaud et al. 2015). Fauna positioned further away from the sediment water interface appeared instead to assimilate other food resources preferentially. These results potentially indicate that macroalgal detritus as a resource enters the benthic food web firstly near the sediment water interface. Once this material has been assimilated and metabolized there, it becomes increasingly difficult to establish how subsequently egested material, or degrading faunal biomass, may lead to the further recycling of macroalgal derived organic matter in sediments. Specifically, using bulk stable isotope signatures, we were unable to ascertain the subsequent processing of this material within the food web, as isotopic signatures may be modified during organic matter decomposition. These two findings (preferential resource uptake at the surface, and uncertainty in isotopic changes during decomposition) may explain

why we found such a small contribution of macroalgae to sedimentary organic carbon stores relative to other organic matter sources, despite the positive carbon fluxes we measured. Indeed, complementing the eDNA analysis, we used bulk stable isotopes as a second biotracing method, applying state-of-the-art Bayesian Stable Isotope Mixing Modeling for the analysis of these data. Importantly, this method allowed us to tackle variability in sources, as measured over the seasonal cycle, as well as unknown sources of error and uncertainty in diet mixes assessed at the benthic community level (Parnell et al. 2013, Stock and Semmens 2016a,b). However, a lack of prior knowledge about the connectivity of the sedimentary study site to shore macroalgae prevented us from using relatively more refined biotracing methods that would have potentially allowed us to trace the material further through the food web, e.g., through the use of fatty acid profiles or compound-specific isotope analysis (Abdullah et al. 2017, Nielsen et al. 2018). Fatty acids are modified in consumers, requiring a priori knowledge of how this process occurs for each source and consumer pair: we did not have this information, and this would have been challenging in a community level study such as this one. In addition, compound specific stable isotope analysis is a relatively newer biotracing approach, and as different compounds may exhibit markedly different integration time in consumers, this technique would have also been difficult to apply in this study (Nielsen et al. 2018). The evidence we uncovered here could guide future work employing these techniques to further resolve the subsequent processing of macroalgal detritus through this food web (and sedimentary stores).

The analysis of bulk stable isotopes requires detailed understanding of the studied system (Phillips et al. 2014), so we took great care in the interpretation of our findings. We sampled potential organic matter sources as comprehensively and accurately as possible, achieving a sound discrimination of sources. Notably, the trophic enrichment we measured between phyto- and zooplankton lends confidence to our plankton sampling methodology (DeNiro and Epstein 1978), as did the general depletion of  $\delta^{13}\text{C}$  from the shore to offshore sources, and the low correlation we found between each of the other sources and SPOM. The latter indicates that, while very small, potentially degrading macroalgae and plankton may have been captured in our SPOM samples, organic matter of different origin was also captured, and this consideration was important in our modeling, given that our study took place near an estuary, influenced by terrestrial runoff (Smyth et al. 2015). Furthermore, while suspension and deposit feeders dominated our faunal communities, carnivores were also part of those communities (SI; meiofaunal community data not shown). Indeed, macrofauna also prey on macro- and meiofauna, and predators in the meiofauna community will prey on meiofauna and on macrofauna larvae. The effects of carnivores on the stable isotopic signature of

macrofauna communities appeared to increase with sediment depth, as reflected in higher average  $\delta^{15}\text{N}$  of macrofauna at depth. However, as macro- and meiofauna were assessed as end consumers at the community level in our Bayesian SIMMs, we were unable to consider benthic fauna as food sources in our analyses. Consequently, our analytical approach did not allow us to discriminate between the uptake of zooplankton and subsurface carnivory, because zooplankton had the most similar isotopic signature to that of higher trophic level benthic fauna. It is thus possible that this may have led to somewhat inflated estimates of zooplankton contributions to benthic diets (as well as to sedimentary organic matter stores).

In the same way that macroalgal life histories were found to affect detritus supply, benthic-pelagic coupling processes driven by sedimentary communities as those measured here (and their natural variation) are determining factors establishing whether detritus available at the seafloor becomes sequestered (Queirós et al. 2015b, Snelgrove et al. 2018). Improving the modeling tools we use to estimate blue carbon sequestration in the coastal and the global ocean must therefore acknowledge that this is a service mediated by oceanic biota, which, in addition to physical processes, affect these and other global carbon fluxes (Snelgrove et al. 2018). This complexity is measurable, and its management not insurmountable, as demonstrated by ecosystem-based management of other sectors affecting marine resources, including fisheries and conservation, more widely.

#### *Net sequestration of organic macroalgal carbon in coastal, deep sediments and other important POC fluxes*

Of the estimated 1,521 Tg C/yr global net primary production of macroalgae, it is estimated that 323 Tg C/yr are exported from shorelines as POC, with 89% of this material assumed to stay in the coastal ocean (reviewed by Krause-Jensen and Duarte 2016). These estimates remain largely unconstrained by field measurements, with few, existing data sets derived predominantly from laboratory studies. Further estimates of what fraction of this carbon are sequestered or re-mineralized coastally are thus largely missing. Based on our 13 month study, we estimate that the average magnitude of net macroalgal POC sequestration at our site is  $0.73 \text{ mol C}\cdot\text{m}^{-2}\cdot\text{yr}^{-1}$  ( $8.75 \text{ g C}\cdot\text{m}^{-2}\cdot\text{yr}^{-1}$ ), as part of a net POC sequestration rate of  $4.89 \text{ mol C}\cdot\text{m}^{-2}\cdot\text{yr}^{-1}$  ( $58.74 \text{ g C}\cdot\text{m}^{-2}\cdot\text{yr}^{-1}$ ). The latter is in line with the estimated average global shelf sea POC flux of  $4.37 \text{ mol C}\cdot\text{m}^{-2}\cdot\text{yr}^{-1}$  (Krumins et al. 2013).

To further constrain the connectivity between sedimentary sites such as ours, and distal macroalgal beds contributing to POC sequestered locally, measurements of detritus production by whole macroalgal communities are needed. These are difficult to come by, and indeed do not exist at present in our study region. However, we were able to compare our estimates with measurements

of detritus production by *L. hyperborea*, which dominates macroalgal standing stocks around Plymouth shores (Pessarrodona et al. 2018). Considering that value ( $100.6\text{--}202.4\text{ g C}\cdot\text{m}^{-2}\cdot\text{yr}^{-1}$ ; Pessarrodona et al. 2018), we estimate that as much as 4–9% of macroalgal POC released annually as detritus from our studied shores may become sequestered in these deep, coastal sediments. These values are relevant in a climate change mitigation context.

Differences between individual study designs (time of year sampled, variation within site) and techniques employed (differences in sensor technology, measurements, setups) may challenge comparisons of this type of studies across the literature. Nevertheless, understanding the role of connected systems within global ocean blue carbon, and the wider carbon cycle, necessitate such an approach, and a focus on (total) net POC fluxes. Accordingly, the net POC flux we measured ( $58.74\text{ g C}\cdot\text{m}^{-2}\cdot\text{yr}^{-1}$ ) equates to 26%, 27%, and 37% of POC fluxes estimated within mangroves, salt marshes, and seagrass beds, respectively; systems more frequently identified as blue carbon habitats (as reviewed by Howard et al. 2017). Our measured macroalgal POC sequestration ( $8.75\text{ g C}\cdot\text{m}^{-2}\cdot\text{yr}^{-1}$ ), representing 15% of the measured net POC sequestration, corresponds to 4–5% of POC fluxes estimated in those other systems (Howard et al. 2017). These values are relevant, given that mangroves, salt marshes, and seagrass beds are readily recognized as important marine carbon sinks, but connected macroalgal-sediment systems are not, and are thus not typically considered under blue carbon conservation efforts (Krause-Jensen et al. 2018). Let us then further consider the UK extension of the type of sedimentary habitat we assessed (European Nature Information System's seabed type A5.25/26, Circalittoral fine sand and muddy-sand, Coates et al. 2016). Taking this extension, we can scale our measurements further to a net flux of  $0.70\text{ Tg C/yr}$  representing the total macroalgal carbon sequestered in this type of habitat in the UK alone. If  $323\text{ Tg C/yr}$  are exported from shorelines globally as particulate organic carbon (as reviewed by Krause-Jensen and Duarte 2016), circalittoral fine sand and muddy-sand in the UK may sequester 0.2% of that organic carbon annually: a non-negligible value. Similarly, we estimate that the net POC sequestered in this type of habitat in the UK is  $4.70\text{ Tg C/yr}$ .

As with any scaling exercise, some uncertainty is associated with the estimates presented here. For instance, we use the annual average of our seasonal measurements; assume, theoretically, that DIC production is entirely fueled by mineralization of macroalgal carbon (or POC); and that carbon sequestration rates are invariable across the habitat we assessed. Furthermore, in these very open, connected systems, natural variation in the processes that determine that connectivity, as well as input and output processes at their boundaries, may provide additional sources of uncertainty, which may be difficult to resolve fully at the ecosystem scale.

Constraining these estimates in similar sedimentary systems in other parts of the globe, with similar field measurements, can provide an important quantitative basis to develop future climate change mitigation policy for a blue carbon scheme that considers connected macroalgal-sedimentary systems (as argued by others; Krause-Jensen et al. 2018). While these systems are not considered, current global efforts to protect vital ocean carbon stores that prevent  $\text{CO}_2$  gas from returning to the atmosphere continue to underestimate the sequestration potential of the coastal ocean. Further measurements of dissolved organic carbon production generated by macroalgal communities, and its potential benthic uptake (which we did not measure) could further increase global significance of the sequestration fluxes we estimate (Krause-Jensen and Duarte 2016).

#### *Managing global blue carbon toward climate change mitigation*

At present, a practical requirement to consider any system as a blue carbon sink within climate change mitigation policies and actions, is the need to provide a means to promote carbon storage above a natural baseline (reviewed by Krause-Jensen et al. 2018, Sutton-Grier and Howard 2018). This is a fundamental aspect that incentivizes practical management solutions within mangroves, seagrass beds, and salt marshes as blue carbon systems, recognized as one-stop donor and sink habitats. However, a wider scope could be seen as a necessary step toward realizing global blue carbon management more widely. Human activities can significantly modify the productivity of macroalgal communities through perturbations of community structure (Lyons et al. 2014, Filbee-Dexter and Scheibling 2016), which, as seen here, has the potential to modify detritus supply regimes. Human activities impacting the soft sediment systems that compose 80% of the ocean floor can also significantly reduce the ability of marine sediments to store organic carbon (Hale et al. 2017). This change can occur as a direct result of physical disturbance to organic carbon stores, or indirectly, through a modification of sedimentary faunal communities that, in addition to physical processes, mediate associated benthic-pelagic carbon fluxes (Queirós et al. 2006, Hale et al. 2017, Snelgrove et al. 2018). Minimizing disturbance to onshore macroalgae and the seafloor through the management of coastal nutrient supply, and of destructive techniques such as bottom fisheries, aggregate extraction, and seabed mining, could therefore have net positive effects on natural blue carbon stores supported by connected macroalgal-sediment systems. That is, benefits could be derived not only from increased storage above a baseline, but rather by limiting activities (managed spatially and temporally) to prevent the degradation of natural processes that otherwise contribute toward the blue carbon provided by connected macroalgal-sediment systems. This perspective is likely to apply

also to other connected blue carbon systems (Hill et al. 2015, Smale et al. 2018). When we consider the sequestration fluxes we measured; that macroalgae are the most productive marine macrophytes globally (Mann 1973, Smith 1981); and the wide distribution of soft sediment beds across the ocean, there is thus real gain to be had in preventing the disturbance of these donor and sink habitats. For connected blue carbon systems to become part of climate change mitigation policies, future research must now aim to provide a stepped improvement in our ability to link specific shore macroalgae communities with seabed detritus accumulation hotspots, e.g., through improved particle tracking modeling or other approaches (Filbee-Dexter and Scheibling 2016). These developments will require improved understanding of how different macroalgal materials are released from the shore (i.e., different species ecologies, different mechanical properties); when and how they degrade; detailed physical modeling of the coastal and open ocean; and an improved ability to model sinking of detritus to the seafloor. Genomic analyses could also be used to robustly match sources of macroalgal DNA on the seafloor to growing populations, as previously done for beach-cast kelp (Fraser et al. 2018). Once hotspots can be identified, targeted carbon flux measurements can be undertaken to quantify net sequestration, including biologically mediated processes, as done here. Given these current gaps in knowledge, mangroves, seagrasses, and salt marshes still presently represent our best bet at managing blue carbon toward climate change mitigation (Sutton-Grier and Howard 2018). And yet, those systems are likely to represent but a fraction of the global blue carbon service delivered by the ocean (Krause-Jensen et al. 2018). Studies such as this one help pave the way for wider global blue carbon accounting and management strategies: these must now strive to include donors as well as sink habitats, and recognize their connectivity.

#### ACKNOWLEDGEMENTS

This work was funded by the Natural Environment Research Council of the UK and the Department for the Environment, Food and Rural Affairs of the UK, through the Marine Ecosystems Research Programme (NE/L003279/1). D. Krause-Jensen thanks the Independent Research Fund Denmark (8021-00222B, "CARMA") for support. The crew of the RV Plymouth Quest is thanked for support during field campaigns. Albert S. Colman (University of Chicago, USA), Andrew Rees (Plymouth Marine Laboratory, UK), Barry Thornton (James Hutton Institute, UK), and Stuart Carter (OEA Labs, UK) are thanked for collaborative development of the stable isotope analysis protocols employed. Gary W. Saunders (University of New Brunswick) is thanked for advice regarding macroalgae barcoding. John Stephens (Plymouth Marine Laboratory) is thanked for advice on the DIC sampling setup. Vas Kitidis is thanked for fruitful discussions on DIC data interpretation. James Fishwick and Oban Jones are thanked for their help in coordinating with the Western Channel Observatory, and support provided accessing that program's data. The bathymetry data used

were sourced from the United Kingdom's Hydrographic Office (UKHO) via the INSPIRE portal (<http://aws2.caris.com/ukho>), under the Open Government Licence version 3.

#### LITERATURE CITED

- Abdullah, M. I., S. Fredriksen, and H. Christie. 2017. The impact of the kelp (*Laminaria hyperborea*) forest on the organic matter content in sediment of the west coast of Norway. *Marine Biology Research* 13:151–160.
- Amaral-Zettler, L. A., E. A. McCliment, H. W. Ducklow, and S. M. Huse. 2009. A method for studying protistan diversity using massively parallel sequencing of V9 hypervariable regions of small-subunit ribosomal RNA genes. *PLoS ONE* 4:e6372.
- Bohmann, K., A. Evans, M. T. P. Gilbert, G. R. Carvalho, S. Creer, M. Knapp, W. Y. Douglas, and M. De Bruyn. 2014. Environmental DNA for wildlife biology and biodiversity monitoring. *Trends in Ecology & Evolution* 29:358–367.
- Burrows, M., N. Kamenos, D. Hughes, H. Stahl, J. Howe, and P. Tett. 2014. Assessment of carbon budgets and potential blue carbon stores in Scotland's coastal and marine environment Project Report. Scottish Natural Heritage, Edinburgh.
- Byers, J. E., and J. H. Grabowski. 2014. Soft-sediment communities. Pages 227–249 in M. D. Bertness, J. F. Bruno, B. R. Silliman and J. J. Stachowicz, editors. *Marine Community Ecology*. Sinauer, Sunderland, Massachusetts, USA.
- Coates, D. A., D. Alexander, R. J. H. Herbert, and S. J. Crowley. 2016. Conceptual ecological modelling of shallow sublittoral sand habitats to inform indicator selection. *JNCC Report* 585.
- Dannheim, J., U. Struck, and T. Brey. 2007. Does sample bulk freezing affect stable isotope ratios of infaunal macrozoobenthos? *Journal of Experimental Marine Biology and Ecology* 351:37–41.
- DeNiro, M. J., and S. Epstein. 1978. Influence of diet on the distribution of carbon isotopes in animals. *Geochimica et Cosmochimica Acta* 42:495–506.
- Dethier, M. N., E. Sosik, A. W. Galloway, D. O. Duggins, and C. A. Simenstad. 2013. Addressing assumptions: variation in stable isotopes and fatty acids of marine macrophytes can confound conclusions of food web studies. *Marine Ecology Progress Series* 478:1–14.
- Duarte, C. M., and J. Cebrián. 1996. The fate of marine autotrophic production. *Limnology and Oceanography* 41:1758–1766.
- Duarte, C. M., I. J. Losada, I. E. Hendriks, I. Mazarrasa, and N. Marbà. 2013. The role of coastal plant communities for climate change mitigation and adaptation. *Nature Climate Change* 3:961–968.
- Filbee-Dexter, K., and R. E. Scheibling. 2016. Spatial patterns and predictors of drift algal subsidy in deep subtidal environments. *Estuaries and Coasts* 39:1724–1734.
- Filbee-Dexter, K., T. Wernberg, K. M. Norderhaug, E. Ramirez-Llodra, and M. F. Pedersen. 2018. Movement of pulsed resource subsidies from kelp forests to deep fjords. *Oecologia* 187:291–304.
- Findlay, H. S., M. A. Kendall, J. I. Spicer, C. Turley, and S. Widdicombe. 2008. Novel microcosm system for investigating the effects of elevated carbon dioxide and temperature on intertidal organisms. *Aquatic Biology* 3:51–62.
- Forster, S., R. N. Glud, J. Gundersen, and M. Huettel. 1999. In situ study of bromide tracer and oxygen flux in coastal sediments. *Estuarine, Coastal and Shelf Science* 49:813–827.
- Fraser, C. I., A. K. Morrison, A. M. Hogg, E. C. Macaya, E. van Sebille, P. G. Ryan, A. Padovan, C. Jack, N. Valdivia,

- and J. M. Waters. 2018. Antarctica's ecological isolation will be broken by storm-driven dispersal and warming. *Nature Climate Change* 8:704.
- Fry, B. 2007. *Stable isotope ecology*. Springer Science & Business Media, New York, New York, USA.
- Gallo, N. D., D. G. Victor, and L. A. Levin. 2017. Ocean commitments under the Paris Agreement. *Nature Climate Change* 7:833.
- Gattuso, J. P., B. Gentili, C. M. Duarte, J. A. Kleypas, J. J. Middelburg, and D. Antoine. 2006. Light availability in the coastal ocean: impact on the distribution of benthic photosynthetic organisms and contribution to primary production. *Biogeosciences Discussions* 3:895–959.
- Gazeau, F., P. van Rijswijk, L. Pozzato, and J. J. Middelburg. 2014. Impacts of ocean acidification on sediment processes in shallow waters of the Arctic Ocean. *PLoS ONE* 9:e94068.
- Glud, R. N. 2008. Oxygen dynamics of marine sediments. *Marine Biology Research* 4:243–289.
- Graham, M. H. 2004. Effects of local deforestation on the diversity and structure of southern California giant kelp forest food webs. *Ecosystems* 7:341–357.
- Hale, R., J. A. Godbold, M. Sciberras, J. Dwight, C. Wood, J. G. Hiddink, and M. Solan. 2017. Mediation of macronutrients and carbon by post-disturbance shelf sea sediment communities. *Biogeochemistry* 135:121–133.
- Hejnowicz, A. P., H. Kennedy, M. A. Rudd, and M. R. Huxham. 2015. Harnessing the climate mitigation, conservation and poverty alleviation potential of seagrasses: prospects for developing blue carbon initiatives and payment for ecosystem service programmes. *Frontiers in Marine Science* 2:32.
- Hill, R., A. Bellgrove, P. I. Macreadie, K. Petrou, J. Beardall, A. Steven, and P. J. Ralph. 2015. Can macroalgae contribute to blue carbon? An Australian perspective. *Limnology and Oceanography* 60:1689–1706.
- Howard, J., A. Sutton-Grier, D. Herr, J. Kleypas, E. Landis, E. Mcleod, E. Pidgeon, and S. Simpson. 2017. Clarifying the role of coastal and marine systems in climate mitigation. *Frontiers in Ecology and the Environment* 15:42–50.
- Hunt, O. D. 1925. The food of the bottom fauna of the Plymouth fishing grounds. *Journal of the Marine Biological Association of the United Kingdom* 13:560–599.
- Knight, M. 1947. A biological study of *Fucus vesiculosus* and *Fucus serratus*. Pages 87–90 in *Proceedings of the Linnean Society of London*. Wiley Online Library.
- Kopp, D., S. Lefebvre, M. Cachera, M. C. Villanueva, and B. Ernande. 2015. Reorganization of a marine trophic network along an inshore–offshore gradient due to stronger pelagic–benthic coupling in coastal areas. *Progress in Oceanography* 130:157–171.
- Krause-Jensen, D., and C. M. Duarte. 2016. Substantial role of macroalgae in marine carbon sequestration. *Nature Geoscience* 9:737–742.
- Krause-Jensen, D., P. S. Lavery, O. Serrano, N. Marba, P. Masque, and C. M. Duarte. 2018. Sequestration of macroalgal carbon: the elephant in the blue carbon room. *Biology Letters* 14:20180236.
- Kristensen, E., G. Penha-Lopes, M. Delefosse, T. B. Valdemarsen, C. O. Quintana, and G. T. Banta. 2012. What is bioturbation? The need for a precise definition for fauna in aquatic sciences. *Marine Ecology-Progress Series* 446:285–302.
- Krumhansl, K. A., and R. E. Scheibling. 2012. Production and fate of kelp detritus. *Marine Ecology Progress Series* 467:281–302.
- Krumins, V., M. Gehlen, S. Arndt, P. V. Cappellen, and P. Regnier. 2013. Dissolved inorganic carbon and alkalinity fluxes from coastal marine sediments: model estimates for different shelf environments and sensitivity to global change. *Biogeosciences* 10:371–398.
- Laffoley, D. 2013. *The management of coastal carbon sinks in Vanuatu: Realising the potential*. Commonwealth Secretariat, London, UK.
- Le Quéré, C., R. M. Andrew, J. G. Canadell, S. Sitch, J. Ivar Korsbakken, G. P. Peters, A. C. Manning, T. A. Boden, P. P. Tans, and R. A. Houghton. 2016. Global carbon budget 2016. *Earth System Science Data* 8:605–649.
- Lessin, G., Y. Artioli, E. Almroth-Rosell, J. C. Blackford, A. Dale, R. N. Glud, J. J. Middelburg, R. Pastres, A. M. Queiros, and C. Rabouille. 2018. Modelling marine sediment biogeochemistry: current knowledge gaps, challenges and some methodological advice for advancement. *Frontiers in Marine Science* 5:19.
- Lüning, K. 1971. Seasonal growth of *Laminaria hyperborea* under recorded underwater light conditions near Helgoland. Pages 347–361 in *Fourth European marine biology symposium*. Cambridge University Press, Cambridge, UK.
- Lyons, D. A., et al. 2014. Macroalgal blooms alter community structure and primary productivity in marine ecosystems. *Global Change Biology* 20:2712–2724.
- Macreadie, P. I., D. A. Nielsen, J. J. Kelleway, T. B. Atwood, J. R. Seymour, K. Petrou, R. M. Connolly, A. C. Thomson, S. M. Trevathan-Tackett, and P. J. Ralph. 2017. Can we manage coastal ecosystems to sequester more blue carbon? *Frontiers in Ecology and the Environment* 15:206–213.
- Mahaut, M., and G. Graf. 1987. A luminophore tracer technique for bioturbation studies. *Oceanologica Acta* 10:323–328.
- Mann, K. H. 1973. Seaweeds—their productivity and strategy for growth. *Science* 182:975–981.
- Mcleod, E., G. L. Chmura, S. Bouillon, R. Salm, M. Björk, C. M. Duarte, C. E. Lovelock, W. H. Schlesinger, and B. R. Silliman. 2011. A blueprint for blue carbon: toward an improved understanding of the role of vegetated coastal habitats in sequestering CO<sub>2</sub>. *Frontiers in Ecology and the Environment* 9:552–560.
- Middelburg, J. 2014. Stable isotopes dissect aquatic food webs from the top to the bottom. *Biogeosciences* 11:2357–2371.
- Middelburg, J. J. 2018. Reviews and synthesis: to the bottom of carbon processing at the seafloor. *Biogeosciences Discussions* 15:413–427.
- Miller, R. J., and H. M. Page. 2012. Kelp as a trophic resource for marine suspension feeders: a review of isotope-based evidence. *Marine Biology* 159:1391–1402.
- Moss, B. 1969. Apical meristems and growth control in *Himantalia elongata* (SF Gray). *New Phytologist* 68:387–397.
- Nellemann, C., E. Corcoran, C. Duarte, L. Valdés, C. De Young, L. Fonseca, and G. Grimsditch. 2009. Blue carbon: A rapid response assessment. *United Nations Environment Programme, GRID-Arendal, Arendal, Norway*.
- Nielsen, J. M., E. L. Clare, B. Hayden, M. T. Brett, and P. Kratina. 2018. Diet tracing in ecology: method comparison and selection. *Methods in Ecology and Evolution* 9:278–291.
- Parke, M. 1948. *Studies on British Laminariaceae. I. Growth in Laminaria saccharina* (L.) Lamour. *Journal of the Marine Biological Association of the United Kingdom* 27:651–709.
- Parnell, A. C., D. L. Phillips, S. Bearhop, B. X. Semmens, E. J. Ward, J. W. Moore, A. L. Jackson, J. Grey, D. J. Kelly, and R. Inger. 2013. Bayesian stable isotope mixing models. *Environmetrics* 24:387–399.
- Pessarrodona, A., P. J. Moore, M. D. Sayer, and D. A. Smale. 2018. Carbon assimilation and transfer through kelp forests in the NE Atlantic is diminished under a warmer ocean climate. *Global Change Biology* 24:4386–4398.
- Phillips, D. L., R. Inger, S. Bearhop, A. L. Jackson, J. W. Moore, A. C. Parnell, B. X. Semmens, and E. J. Ward. 2014.

- Best practices for use of stable isotope mixing models in food-web studies. *Canadian Journal of Zoology* 92:823–835.
- Polis, G. A., W. B. Anderson, and R. D. Holt. 1997. Toward an integration of landscape and food web ecology: the dynamics of spatially subsidized food webs. *Annual Review of Ecology, Evolution, and Systematics* 28:289–316.
- Queirós, A. M., J. G. Hiddink, M. J. Kaiser, and H. Hinz. 2006. Effects of chronic bottom trawling disturbance on benthic biomass, production and size spectra in different habitats. *Journal of Experimental Marine Biology and Ecology* 335:91–103.
- Queirós, A. M., P. Taylor, A. Cowles, A. Reynolds, S. Widdicombe, and H. Stahl. 2015. Optical assessment of impact and recovery of sedimentary pH profiles in ocean acidification and carbon capture and storage research. *International Journal of Greenhouse Gas Control* 38:110–120.
- Queirós, A. M., et al. 2015a. Scaling up experimental ocean acidification and warming research: from individuals to the ecosystem. *Global Change Biology* 21:130–143.
- Queirós, A. M., et al. 2015b. Can benthic community structure be used to predict the process of bioturbation in real ecosystems? *Progress in Oceanography* 137:559–569.
- Regnier, P., P. Friedlingstein, P. Ciais, F. T. Mackenzie, N. Gruber, I. A. Janssens, G. G. Laruelle, R. Lauerwald, S. Luysaert, and A. J. Andersson. 2013. Anthropogenic perturbation of the carbon fluxes from land to ocean. *Nature Geoscience* 6:597–607.
- Renaud, P. E., T. S. Løkken, L. L. Jørgensen, J. Berge, and B. J. Johnson. 2015. Macroalgal detritus and food-web subsidies along an Arctic fjord depth-gradient. *Frontiers in Marine Science* 2:31.
- Reygondeau, G., J. C. Molinero, S. Coombs, B. R. MacKenzie, and D. Bonnet. 2015. Progressive changes in the Western English Channel foster a reorganization in the plankton food web. *Progress in Oceanography* 137:524–532.
- Rieper-Kirchner, M. 1990. Macroalgal decomposition: laboratory studies with particular regard to microorganisms and meiofauna. *Helgoländer Meeresuntersuchungen* 44:397.
- Schiffers, K., L. R. Teal, J. Mark, J. Travis, and M. Solan. 2011. An open source simulation model for soil and sediment bioturbation. *PLoS ONE* 6:e28028.
- Sjotun, K. 1995. Adaptive aspects of growth and reproduction in two North Atlantic *Laminaria* species. University of Bergen, Bergen, Norway.
- Smale, D., and T. Vance. 2015. Climate-driven shifts in species' distributions may exacerbate the impacts of storm disturbances on North-east Atlantic kelp forests. *Marine and Freshwater Research* 67:65.
- Smale, D. A., P. J. Moore, A. M. Queiros, N. D. Higgs, and M. T. Burrows. 2018. Appreciating interconnectivity between habitats is key to Blue Carbon management. *Frontiers in Ecology and the Environment* 16:71–73.
- Smith, S. 1981. Marine macrophytes as a global carbon sink. *Science* 211:838–840.
- Smyth, T., A. Atkinson, S. Widdicombe, M. Frost, J. Allen, J. Fishwick, A. Queirós, D. Sims, and M. Barange. 2015. The western channel observatory. *Progress in Oceanography* 137:335–341.
- Snelgrove, P. V., K. Soetaert, M. Solan, S. Thrush, C.-L. Wei, R. Danovaro, R. W. Fulweiler, H. Kitazato, B. Ingole, and A. Norrko. 2018. Global Carbon Cycling on a Heterogeneous Seafloor. *Trends in Ecology & Evolution* 33:96–105.
- Stock, B., and B. Semmens. 2016a. MixSIAR GUI User Manual v3.1. Scripps Institution of Oceanography, UC San Diego, San Diego, California, USA.
- Stock, B. C., and B. X. Semmens. 2016b. Unifying error structures in commonly used biotracer mixing models. *Ecology* 97:2562–2569.
- Sutton-Grier, A., and J. Howard. 2018. Coastal wetlands are the best marine carbon sink for climate mitigation. *Frontiers in Ecology and the Environment* 16:73–74.
- Tait, K., R. L. Airs, C. E. Widdicombe, G. A. Tarran, M. R. Jones, and S. Widdicombe. 2015. Dynamic responses of the benthic bacterial community at the Western English Channel observatory site L4 are driven by deposition of fresh phytodetritus. *Progress in Oceanography* 137:46–558.
- Tenzer, R., and V. Gladkikh. 2014. Assessment of Density Variations of Marine Sediments with Ocean and Sediment Depths. *The Scientific World Journal* 2014:9. <https://doi.org/10.1155/2014/823296>
- Wada, E., H. Mizutani, and M. Minagawa. 1991. The use of stable isotopes for food web analysis. *Critical Reviews in Food Science & Nutrition* 30:361–371.
- Waldron, S., E. Marian Scott, L. E. Vihermaa, and J. Newton. 2014. Quantifying precision and accuracy of measurements of dissolved inorganic carbon stable isotopic composition using continuous-flow isotope-ratio mass spectrometry. *Rapid Communications in Mass Spectrometry* 28:1117–1126.
- Weiss, R. 1970. The solubility of nitrogen, oxygen and argon in water and seawater. *Deep Sea Research and Oceanographic Abstracts* 17:721–735.
- Zhang, Q., R. M. Warwick, C. L. McNeill, C. E. Widdicombe, A. Sheehan, and S. Widdicombe. 2015. An unusually large phytoplankton spring bloom drives rapid changes in benthic diversity and ecosystem function. *Progress in Oceanography* 137:533–545.

## SUPPORTING INFORMATION

Additional supporting information may be found online at: <http://onlinelibrary.wiley.com/doi/10.1002/ecm.1366/full>

## DATA AVAILABILITY

The eDNA sequence data generated in this study are publicly available at the National Center for Biotechnology Information (USA) via the SRA accession number SRP148635. The remaining data supporting the results are archived in the British Oceanographic Data Centre at <https://doi.org/10.5285/80856b3b-24df-4e53-e053-6c86abc0ed2b>.